

Highlights

► In cockroaches, juvenile hormone induces the expression of Broad complex in young stages ► In flies, juvenile hormone inhibits its expression of Broad complex in young stages ► In cockroaches, Broad complex promote wing growth and patterning ► In flies, it specifies pupal morphogenesis ► Broad complex played a key role in metamorphosis evolution from cockroaches to flies

1 *Broad-complex* functions in postembryonic development of the cockroach *Blattella*
2 *germanica* shed new light on the evolution of insect metamorphosis

3

4 Jia-Hsin Huang ^{a, b} Jesus Lozano ^a and Xavier Belles ^{a, *}

5

6 ^a Institute of Evolutionary Biology (CSIC-Universitat Pompeu Fabra), Passeig Marítim
7 de la Barceloneta 37, 08003 Barcelona, Spain

8 ^b Permanent address: Department of Entomology, National Taiwan University, Taipei
9 106, Taiwan

10

11

12 * Corresponding author at: Institute of Evolutionary Biology (CSIC-UPF), Passeig
13 Marítim de la Barceloneta 37, 08003 Barcelona, Spain. Tel.: +34 932309636; fax: +34
14 932211011. E-mail address: xavier.belles@ibe.upf-csic.es (X. Belles).

15

16 *Key Words:*

17 Insect metamorphosis

18 juvenile hormone

19 ecdysone

20 evolution of holometaboly

21 *Drosophila*

22 *Tribolium*

23 cockroach

24

25 ABSTRACT

26 *Background:* Insect metamorphosis proceeds in two modes: hemimetaboly, gradual
27 change along the life cycle, and holometaboly, abrupt change from larvae to adult
28 mediated by a pupal stage. Both are regulated by 20-hydroxyecdysone (20E), which
29 promotes molts, and juvenile hormone (JH), which represses adult morphogenesis.
30 Expression of Broad complex (BR-C) is induced by 20E and modulated by JH. In
31 holometabolous species, like *Drosophila melanogaster*, BR-C expression is inhibited by
32 JH in young larvae and enhanced in mature larvae, when JH declines and BR-C
33 expression specifies the pupal stage.

34 *Methods:* Using *Blattella germanica* as a basal hemimetabolous model, we determined
35 the patterns of expression of BR-C mRNAs using quantitative RT-PCR, and we studied
36 the functions of BR-C factors using RNA interference approaches.

37 *Results:* We found that BR-C expression is enhanced by JH and correlates with JH
38 hemolymph concentration. BR-C factors appear involved in cell division and wing pad
39 growth, as well as wing vein patterning.

40 *Conclusions:* In *B. germanica*, expression of BR-C is enhanced by JH, and BR-C
41 factors appear to promote wing growth to reach the right size, form and patterning,
42 which contrast with the endocrine regulation and complex functions observed in
43 holometabolous species.

44 *General significance:* Our results sheds new light to the evolution from hemimetaboly
45 to holometaboly regarding BR-C, whose regulation and functions were affected by two
46 innovations: 1) a shift in JH action on BR-C expression during young stages, from
47 stimulatory to inhibitory, and 2) an expansion of functions, from regulating wing
48 development, to determining pupal morphogenesis.

49

50 **1. Introduction**

51 The origin and evolution of insect metamorphosis poses one of the most
52 enigmatic conundrums in evolutionary biology. In his “On the Origin of Species”,
53 Charles Darwin already complained about the difficulty of integrating insect
54 metamorphosis (due to the striking difference between the morphologies and life styles
55 of larvae and adults of the same species) into his theory of species evolution by natural
56 selection [1]. However, it is clear that insect metamorphosis has been a key innovation
57 in insect evolution as most of the present biodiversity on Earth is composed of
58 metamorphosing insects, with approximately 1 million species described, and 10-30
59 million still to be discovered [2, 3].

60 The first systematic studies on insect metamorphosis were carried out by
61 Renaissance entomologists, who established that post-embryonic changes are most
62 spectacular in insects like butterflies, beetles and flies, which undergo a dramatic
63 morphological transformation from larva to pupa and adult, a phenomenon now known
64 as holometaboly. Other insects, such as locusts and cockroaches, also metamorphose
65 from the last nymphal instar to adult, although the change of form is not as radical given
66 that the nymphs are similar to the adults. However, they undergo qualitative
67 metamorphic changes, such as formation of mature wings and external genitalia in a
68 type of metamorphosis known as hemimetaboly [4, 5]. Metamorphosis evolved from
69 hemimetaboly to holometaboly, and the latter innovation was most successful because
70 more than 80% of present insects are holometabolous species (including the “big four”
71 orders: Lepidoptera, Coleoptera, Diptera and Hymenoptera) [2, 3]. Therefore,
72 explaining the evolutionary transition from hemimetaboly to holometaboly may give a
73 new look to explain how this amazing biodiversity originated, and the study of the
74 processes regulating metamorphosis shall surely provide important clues for such a goal
75 [6].

76 Insect metamorphosis is regulated by two hormones, the molting hormone,
77 which promotes molting, and the juvenile hormone (JH), which represses
78 metamorphosis and, thus determines the molt type: to an immature stage when it is
79 present, or to the adult when it is absent [4, 6, 7]. Although the molecular action of JH is
80 still poorly understood [8], we know that an important transducer of the JH signal is
81 Methoprene tolerant (Met), a transcription factor that was discovered in *Drosophila*
82 *melanogaster* and that plays an important role in JH reception [9]. Key functional

83 evidence that Met is required for the repressor action of JH on metamorphosis was
84 obtained from the beetle *Tribolium castaneum*, a basal holometabolous insect where
85 depletion of Met expression induced larvae to undergo precocious metamorphosis [10,
86 11]. More recently, the function of Met as an early JH transducer has been demonstrated
87 in the hemimetabolous species *Pyrrhocoris apterus* [12], which established the first
88 regularity in the signaling pathway of JH in hemimetabolous and holometabolous
89 insects. Another important element in JH transduction in relation to metamorphosis is
90 the transcription factor Krüppel homolog 1 (Kr-h1), whose antimetamorphic action was
91 firstly demonstrated in *D. melanogaster* [13] and *T. castaneum* [14]. More recently, the
92 role of Kr-h1 as a transducer of the JH signal has been reported in three
93 hemimetabolous insects: the cockroach *Blattella germanica* [15] and the bugs *P. apterus*
94 and *Rhodnius prolixus* [12]. RNAi studies in these species have shown that Kr-h1
95 represses metamorphosis and that it acts downstream of Met in the JH signaling
96 pathway. Kr-h1 therefore appears to be the more distal transcription factor in the JH
97 signaling cascade whose role as mediator of the antimetamorphic action of JH has been
98 conserved from cockroaches to flies. The next challenge is to unveil the factor(s)
99 specifying the adult stage that are repressed by Kr-h1.

100 Concerning the molecular action of molting hormones, the effect of 20-
101 hydroxyecdysone (20E) is also mediated by a cascade of transcription factors that starts
102 upon its binding to the heterodimeric receptor composed of the ecdysone receptor and
103 the ultraspiracle, which belong to the nuclear receptor superfamily. This activates
104 expression of a hierarchy of transcription factors generally belonging to the same
105 superfamily, like E75, E78, HR3, HR4 and FTZ-F1, which regulate the genes that
106 underlie the cellular changes associated to molting and metamorphosis [16, 17]. Most of
107 the information available on this cascade refers to *D. melanogaster* [18, 19], but there
108 are a good deal of data from hemimetabolous species, especially from the cockroach *B.*
109 *germanica*. Factors involved in 20E signaling in *B. germanica* are generally the same as
110 in *D. melanogaster*, although the functions of some of them and their epistatic
111 relationships may differ with respect to those observed in the fly [20-22].

112 Among the most interesting 20E-dependent factors are the products of the Broad
113 complex (BR-C) gene, whose functions may have radically diverged in hemimetabolous
114 and holometabolous species. BR-C encodes a group of C2H2 zinc-finger transcription
115 factors [23, 24] that, in holometabolous species, like the dipteran *D. melanogaster*, the

116 lepidopterans *Manduca sexta* and *Bombyx mori*, and the coleopteran *T. castaneum*, are
117 expressed in the final larval stage, and this transient expression is essential for the
118 successful formation of the pupae [11, 25-28]. Experiments carried out on the
119 hemipterans *Oncopeltus fasciatus* [29] and *P. apterus* [12], which are phylogenetically
120 distal hemimetabolous species, suggested that BR-C transcription factors only regulate
121 gradual wing bud growth. This specific role, which is radically different from the
122 morphogenetic functions involved in pupae formation in holometabolous species,
123 prompted us to undertake a detailed functional study of BR-C in *B. germanica*, a basal
124 polyneopteran insect representing a poorly modified hemimetabolous species [4]. In *B.*
125 *germanica*, the BR-C gene encodes six zinc-finger isoforms (BR-C Z1 to Z6), which
126 play important roles in embryogenesis [30]. The present work, based on functional
127 studies in post-embryonic development, reveals ancestral functions of BR-C
128 transcription factors related to cell division and of wing pad growth, as well as to wing
129 vein patterning, and provides new clues that illuminate the evolution of insect
130 metamorphosis.

131

132 **2. Materials and methods**

133 *2.1. Insects*

134 *B. germanica* specimens used in the experiments were obtained from a colony
135 reared in the dark at $30 \pm 1^\circ\text{C}$ and 60-70% r.h. They were carbon dioxide-anaesthetized
136 prior to dissections and tissue sampling.

137

138 *2.2. RNA Extraction and retrotranscription to cDNA*

139 All RNA extractions were carried out with the Gen Elute Mammalian Total RNA
140 kit (Sigma-Aldrich, Madrid, Spain). An amount of 400 ng from each RNA extraction
141 was treated with DNase (Promega, Madison, WI, USA) and reverse transcribed with
142 Superscript II reverse transcriptase (Invitrogen, Carlsbad CA, USA) and random
143 hexamers (Promega). RNA quantity and quality was estimated by spectrophotometric
144 absorption at 260 nm in a Nanodrop Spectrophotometer ND-1000® (NanoDrop
145 Technologies, Wilmington, DE, USA).

146

147 *2.3. Determination of mRNA levels with quantitative real-time PCR*

148 Quantitative real time PCR (qRT-PCR) reactions were carried out in triplicate in
149 an iQ5 Real-Time PCR Detection System (Bio-Rad Laboratories, Madrid, Spain), using
150 SYBR®Green (Power SYBR® Green PCR Master Mix; Applied Biosystems, Madrid,
151 Spain). A control without template was included in all batches. The primers used to
152 detect all isoforms simultaneously or to detect each isoform specifically are described in
153 Table S1 (see Supplementary data). The efficiency of each primer set was first validated
154 by constructing a standard curve through four serial dilutions. mRNA levels were
155 calculated relative to BgActin- 5c (Accession number AJ862721) expression using the
156 Bio-Rad iQ5 Standard Edition Optical System Software (version 2.0). The primers used
157 to quantify BgActin-5c are indicated in Table S2 (see Supplementary data). We
158 followed a method based in Ct (threshold-cycle) according to the Pfaffl mathematical
159 model [31], simplifying to $2^{\Delta\Delta Ct}$ because the calculated efficiency values for studied
160 genes and BgActin-5c amplicons were always within the range of 95 to 100%;
161 therefore, no correction for efficiency was used in further calculations. Results are given
162 as copies of mRNA per 1,000 copies of BgActin-5c mRNA.

163

164 *2.4. Treatments with juvenile hormone III in vivo*

165 To study the effect of JH upon BR-C expression, JH III, which is the native JH
166 of *B. germanica* [32, 33], was applied topically to freshly emerged last instar nymphs at
167 a dose of 20 µg per specimen in 1 µl of acetone. We used JH III from Sigma-Aldrich,
168 which is a mixture of isomers containing about 50% of the biologically active (10R)-JH
169 III. Thus, the active dose applied would be around 10 µg per specimen, which is an
170 efficient dose to impair metamorphosis [34]. Controls received 1 µl of acetone.

171

172 *2.5. RNA interference*

173 *B. germanica* is very sensitive to RNA interference (RNAi) in vivo [35].
174 Detailed procedures for dsRNA preparation and RNAi experiments were as described
175 previously [22, 36, 37]. Concerning BR-C, dsRNAs were prepared to deplete all
176 isoforms simultaneously (dsBrCore) or specific isoforms BR-C Z1 to BR-C Z6 (dsBrZ1
177 to dsBrZ6). The primers used to generate templates with PCR for transcription of these
178 dsRNAs are described in Table S3 (see Supplementary data). The fragments were
179 amplified by PCR and cloned into the pSTBlue-1 vector (Novagen, Madrid, Spain). In

180 all cases, we used a 307 bp sequence from *Autographa californica* nucleopolyhydro-
181 virus (Accession number K01149, from nucleotide 370 to 676) as control dsRNA
182 (dsMock). A volume of 1 µl of each dsRNA solution (3 µg/µl) was injected into the
183 abdomen of specimens at chosen ages and stages. Control specimens were treated with
184 the same dose and volume of dsMock. RNAi of Kr-h1 was carried out as recently
185 reported [15].

186

187 *2.6. Wing morphological studies*

188 Development of mesonotum and metanotum wing primordia or wing buds was
189 studied in 5th (N5, penultimate) and 6th (N6, last) nymphal instars. Wing buds were
190 exposed out of the dorsal cuticular layer under Ringer's saline. Then, they were fixed in
191 4% paraformaldehyde and permeabilised in PBS-0.2% tween (PBT), incubated for 20
192 min in 300 ng/ml phalloidin-Tetramethyl Rhodamine Isothiocyanate (Sigma-Aldrich) in
193 PBT, rinsed with PBS, and stained for 10 min in 1 µg/ml DAPI in PBT. After three
194 washes with PBT, the wing buds were mounted in Mowiol 4-88 (Calbiochem), and were
195 examined by epifluorescence microscopy AxioImager.Z1 (ApoTome System, Zeiss).
196 Adult forewings (tegmina) and hindwings (membranous) were studied and
197 photographed first in the intact animal, and then dissected out, mounted on a slide with
198 Mowiol 4-88. In these cases, examinations and photographs were made with a
199 stereomicroscope Zeiss DiscoveryV8. Biometrical measurements of wing size
200 parameters were carried out with an ocular micrometer adapted to this
201 stereomicroscope.

202

203

204 *2.7. EdU experiments to measure cell proliferation in vivo*

205 EdU (5-ethynyl-2'-deoxyuridine) is a thymidine analogue recently developed for
206 labeling DNA synthesis and dividing cells in vitro [38], which is more sensitive and
207 practical than the commonly used 5-bromo-2'-deoxyuridine, BrdU. We followed an
208 approach in vivo, using used the commercial EdU compound "Click-it EdU-Alexa
209 Fluor[®] 594 azide" (Invitrogen, Molecular Probes), which was applied topically on the
210 first abdominal tergites (10 µg in 1 µl of DMSO) of staged nymphs. Control specimens
211 received 1 µl of DMSO. Wing buds from treated specimens were dissected 24 h later,
212 and processed for EdU detection according to the manufacturer's protocol.

213

214 2.8. Statistics

215 In general, data are expressed as mean \pm standard error of the mean (SEM). In
216 qRT-PCR determinations, statistical analyses between groups were tested by the REST
217 2008 program (Relative Expression Software Tool V 2.0.7; Corbett Research) [39]. This
218 program makes no assumptions about the distributions, evaluating the significance of
219 the derived results by Pair-Wise Fixed Reallocation Randomization Test tool in REST
220 [39]. Statistical analyses of wing biometrical measurements were carried out with the
221 Student's *t*-test.

222

223

224 3. Results

225 3.1. Broad complex isoforms are expressed along the entire nymphal life of *B.*

226 *germanica*

227 As a first step in our work, we studied the temporal expression of BR-C during
228 the nymphal life of the cockroach *B. germanica*. Firstly, we used whole body extracts
229 and a primer set amplifying a fragment in the core region of BR-C, which is common to
230 the six BR-C isoforms. Results obtained show that BR-C transcripts are present in the
231 six nymphal instars (N1 to N6) at levels of some 100 copies per 1,000 copies of actin
232 mRNA. In the last nymphal instar (N6), BR-C mRNA levels steadily decreased until
233 becoming practically undetectable just before molting to the adult stage (Fig. 1A).

234 Given that BR-C functions in hemimetabolous insects appeared to be associated
235 to wing growth, we obtained expression patterns in the pooled wing pads, that is, the
236 lateral expansions of the mesonotum and metanotum, which contain the wing buds,
237 during the last two nymphal instars (N5 and N6). Results revealed that BR-C is highly
238 expressed in wing pads in N5, the expression levels forming a peak on day 4. In N6 the
239 expression levels are notably lower and steadily decreasing, although showing a small
240 peak of expression on day 6 (Fig. 1B). The expression peaks in N5 and N6 correspond
241 to the peaks of 20E, and the high levels of expression in N5 correlate with the presence
242 of JH, while the levels decrease in N6 when JH vanishes (Fig. 1B, *bottom*).

243 The expression of the individual isoforms, BR-C Z1 to BR-C Z6 in the wing
244 pads during N6 show the same pattern in all isoforms: high levels at emergence, then a
245 steady decrease although with a small peak of expression on day 6 (Fig. 1C). Moreover,
246 the study shows that BR-C Z2 is the most abundant isoform, followed by Z3, Z6, Z4,

247 Z1 and Z5. With the RNA extract used to study the individual isoforms (results in Fig.
248 1C) we also amplified the core region fragment as in Fig. 1A. The mRNA values
249 obtained were similar to those resulting from the sum of values of all isoforms for each
250 day (Supplementary Fig. S1), which suggests that the six BR-C isoforms known in *B.*
251 *germanica* constitute the complete functional set.

252 As stated above, the dramatic differences of BR-C expression between N5 and
253 N6 are probably due to JH, which is abundantly present in N5 and practically absent in
254 N6. This suggests that JH enhances the expression of BR-C in *B. germanica*, and that
255 the decline of BR-C mRNA levels in N6 may largely be due to the absence of JH. In
256 agreement with this, topical treatment of freshly emerged N6 with 20 μ g of JH III
257 induced the re-expression of BR-C (Fig. 1D). Congruently, depletion of Kr-h1, a
258 transcription factor involved in early JH signaling, decreases BR-C expression levels in
259 N4 and in N5 (Fig. 1E).

260

261 3.2. BR-C depletion impairs wing development

262 To study the role of BR-C, cockroaches were treated with 3 μ g dsRNA targeting
263 the core region of BR-C (dsBrCore) at day 0 of N5. Controls were equivalently treated
264 with dsMock. On day 6 of N5 and on day 0 of N6, levels of BR-C mRNA in dsBrCore-
265 treated specimens were significantly lower than those measured in controls (Fig. 2A).
266 dsBrCore-treated specimens (n = 34) molted normally to N6, but the adults emerging
267 from the subsequent molt showed a number of differences with respect to dsMock-
268 treated controls (n = 24). In dsBrCore-treated specimens, both wing pairs were well
269 extended, but the forewings appeared to be somewhat broader and the hindwings were
270 smaller than those of the controls, and showed a number of vein defects (Fig. 2B).
271 Biometrical data supported the observations regarding form and size (Supplementary
272 Fig. S2). And as to the hind wing vein patterning, 19 out of 34 specimens (56%) had the
273 CuP vein shorter and an associated notch at the wing edge (defect A, Supplementary
274 Fig. S3); four specimens (12%) showed vein/intervein pattern disorganization in the
275 anterior part of the wing (defect B, Supplementary Fig. S3); six specimens (17%)
276 showed the defects A and B; and five specimens (15%) had A and B defects and their A-
277 veins were subdivided and incomplete (defect C, Supplementary Fig. S3). In all other
278 respects, the external morphology of the adult of dsBrCore-treated specimens was
279 normal. Control (dsMock-treated) specimens developed normally patterned wings,
280 although a small percentage of the specimens (3 out of 24, 12.5%) showed the defect B

281 (Supplementary Fig. S3).

282 We then increased the RNAi effectiveness using two doses of 3 μ g of dsBrCore,
283 administered respectively on days 0 and 3 of N5. Levels of BR-C mRNA measured on
284 day 6 of N5 (Fig. 2C) were lower than those obtained with a single injection (Fig. 2A).
285 Specimens treated twice with dsBrCore (n = 23) molted normally to N6, and then to the
286 adult stage, which showed malformed wings. About 70% of the adult specimens (16 out
287 of 23) showed a phenotype similar to that obtained with a single injection of dsRNA:
288 the wings being well extended but with the typical notch produced by a shortening of
289 the CuP vein, a similar diversity of vein patterning malformations, and with broader
290 forewings and smaller hindwings than in controls (Fig. 2D, *left*). The remaining 30%
291 exhibited a wing phenotype more severe, with the forewings and hindwings heavily
292 reduced and so wrinkled (Fig. 2D, *right*) that it was difficult to extend them on a slide;
293 however, close examination indicated that all of them had the A, B and C vein defects
294 observed in the dsBrCore-treated specimens that emerged with the wings well extended.
295 Arguably, differences in severity of the effects are due to differences of penetrance and
296 intrinsic variability in these experiments. All the controls treated equivalently with two
297 doses of dsMock (n = 18) emerged with normal wings in terms of size, form and vein
298 patterning.

299 In order to assess whether BR-C could play a role on the wing development of
300 younger instars, we administered two doses (3 μ g-each) of dsBrCore on days 0 and 3
301 respectively of N4. On day 0 of N5, levels of BR-C mRNA in dsBrCore-treated
302 specimens were significantly lower than controls (dsMock-treated) (Fig. 2E). dsBrCore-
303 treated specimens (n = 22) molted normally to N5 and to N6, but when molting to the
304 adult stage they showed the wing malformations observed in the former experiments,
305 with extended and wrinkled wing phenotypes, but with a higher proportion of the latter.
306 Thus, only six out of 22 treated specimens (27%) showed the extended wing phenotype,
307 and even these had the wings imperfectly extended (Fig. 2F, *left*); moreover, the wings
308 exhibited the A, B and C defects and reduced size typical of BR-C knockdowns. The
309 remaining 16 specimens (73%) showed the more severe wrinkled wing phenotype (Fig.
310 2F, *right*). Controls (dsMock-treated, n = 21), had normal wing patterning, except three
311 specimens (14.3%) that exhibited the B defect.

312 Finally, we aimed at studying the effect of BR-C depletion in the last instar
313 nymph (N6), where the transition to the adult stage occurs. Cockroaches were treated
314 with two doses of 3 μ g each of dsBrCore, one administered on day 0 and the other on

315 day 3 of N6. Three days later (day 6), levels of BR-C mRNA were significantly lower in
316 dsBrCore-treated insects than in controls (Fig. 2G). All adults obtained after this
317 treatment (n = 24) emerged with the wings well extended, and only 5 of them (21%)
318 showed the A defect (Fig. 2H, *right*). Control (dsMock-treated) specimens (n = 23) had
319 normal wing patterning, and only one specimen (4%) had the B defect (Fig. 2H, *left*).
320

321 *3.3. BR-C depletion impairs cell division in wing buds*

322 The decrease in wing size, especially in the hindwings, suggests that there was a
323 problem of cell proliferation in dsBrCore-treated specimens. To test this possibility, we
324 first studied cell division in the hindwing buds in N6 around the peak of 20E, which
325 takes place between days 5 and 7, with maximum values on day 6 [40]. Cell division in
326 the hindwing buds, which are located within a pocket in the lateral expansions of the
327 metanotum, was labeled with EdU. On day 5, EdU labeling revealed intense cell
328 division on the surface of the hindwing bud (Fig. 3A, *day 5*). On day 6, cell division on
329 the surface practically vanished, while the wing bud started growing and folding (Fig.
330 3A, *day 6*). Towards the end of day 6 and during the whole of day 7, EdU labeling
331 disappeared and a remarkable, general wing growth took place, that provoked multiple
332 and thick folds on the hindwing surface (Fig. 3A, *day 7*). The same transition from cell
333 division to wing growth between days 5 and 7 occurs in the forewing buds (Fig. 3B,
334 *control*), which are located within the lateral expansions of the mesonotum.

335 In specimens treated with a double dose of 3 μ g of dsBrCore administered
336 respectively on days 0 and 3 of N5, EdU labeling in the forewing buds on day 5 of N6
337 was significantly reduced in comparison with controls (dsMock-treated) (Fig. 3B, *left*
338 *panels, compare control and treated*). On day 6, during the period of growth and folding
339 in controls, remarkable surface reduction was noticed along the edges of the wing pad in
340 dsBrCore-treated specimens (Fig. 3B, *right panels, compare control and treated*), which
341 parallels the statistically significant reduction on wing size measured after the imaginal
342 molt (Supplementary Fig. S2). Concerning the hindwing buds, EdU labeling on day 5
343 was also more reduced in the specimens treated with dsBrCore than in controls treated
344 with dsMock. Differences were particularly obvious at the distal end of the CuP vein,
345 where EdU labeling was practically absent in dsBrCore-treated specimens, in comparison
346 with controls (Fig. 3C). Interestingly, the distal end of the CuP vein, where there is no
347 cell division, disappeared thereafter, on day 6, at the maximum peak of ecdysone,
348 therefore forming the characteristic notch of the BR-C knockdowns (Fig. 2B, D, F, H

349 and Supplementary Fig. S3). In the subsequent stage of tissue growth without cell
350 division, from the end of day 6 to the ecdysis, on day 8, differences between dsBrCore-
351 treated specimens and controls were not apparent in either the forewing or the hindwing
352 buds. We also used EdU labeling to study wing bud cell division around the 20E peak of
353 N5 in specimens that had been treated with two doses of dsBrCore on days 0 and 3 of
354 N4. Results showed that cell division was lower in dsBRCore-treated specimens than in
355 controls (dsMock-treated), both in the forewing and in the hindwing buds (results not
356 shown), as occurred in N6.

357

358 *3.4. Functions of individual BR-C isoforms in B. germanica*

359 All BR-C isoforms, from Z1 to Z6, are expressed simultaneously, although at
360 different levels, and show the same pattern (Fig. 1C), suggesting that all of them
361 contribute to the same functions in post-embryonic development. However, we aimed to
362 test this conjecture by carrying out isoform-specific RNAi experiments on all isoforms.
363 Treatments were carried out in N5, by injecting two doses of 3 µg of the corresponding
364 BR-C dsRNA (dsBrZ1 to dsBrZ6), one on day 0 and the other on day 3. Controls were
365 equivalently treated with dsMock.

366 Transcript depletion of the specifically targeted isoform was measured on the
367 wing pads on day 0 of N6. Transcript levels of all other non-targeted isoforms were also
368 measured as a control of RNAi specificity. Results (Fig. 4A-F) show that, in general,
369 individual isoform RNAi experiments were isoform-specific in terms of transcript
370 depletion. Treatment with dsBrZ3 reduced BR-C Z3 mRNA levels, but differences with
371 respect to the corresponding controls were not statistically significant. This treatment
372 also tended to reduce BR-C Z2 mRNA levels and, intriguingly, tended to increase the
373 mRNA levels of BR-C Z4, BR-C Z5 and BR-C Z6 (Fig. 4B). It is also worth noting that
374 treatment with dsBrZ4 significantly reduced BR-C Z4 mRNA levels, as expected, but
375 also those of BR-C-Z5 (Fig. 4D).

376 In terms of phenotype, all specimens in all isoform-specific RNAi experiments
377 molted normally to N6 and then to adult. A detailed examination of the external
378 morphology of the adult was then performed and differences with respect to controls
379 were only noticed in the wings of specimens treated with dsBrZ2 and dsBrZ6.
380 Concerning dsBrZ2-treated specimens (n = 27), 18 of them (67%) had only the A defect
381 (Fig. 4G); 1 (4%) showed only the B defect; and 7 (26%) had no visible defects. No
382 significant differences were observed in wing sizes between treated specimens and

383 controls, neither in the hindwing nor the forewing. The hindwing phenotype resembles
384 that obtained when depleting all isoforms simultaneously, but less marked, with less
385 penetrance and without the C defect (see Supplementary Fig. S3). All control (dsMock-
386 treated) specimens (n = 12) showed normal wing patterning except one specimen (8%)
387 that had the B defect. In the dsBrZ6-treated group (n = 25), 9 specimens (36%) showed
388 the B defect (Fig. 4H), whereas the remaining 16 were perfectly patterned. In the
389 control group (dsMock-treated) (n = 18), 2 specimens (11%) showed the B defect.

390 Specimens obtained from RNAi experiments targeting Z1 (dsBrZ1-treated, n =
391 18; dsMock-treated, n = 10), Z3 (dsBrZ3-treated, n = 24; dsMock-treated, n = 14), Z4
392 (dsBrZ4-treated, n = 16; dsMock-treated, n = 11) and Z5 (dsBrZ5-treated, n = 18;
393 dsMock-treated, N=10), had the wings well extended and correctly patterned (Fig. 4I),
394 and only a few specimens (between 0 and 14%, irrespective of the group, either in
395 treated or controls) had the B defect.

396

397 **4. Discussion**

398 *4.1. The patterns and the hormonal environment*

399 In *B. germanica*, BR-C isoforms are expressed in all nymphal stages, and
400 expression only declines in the last, pre-imaginal stage. The expression pattern is similar
401 in all individual isoforms of BR-C, although the respective abundances differ, Z2 being
402 the most abundant, followed by Z3, Z6, Z4, Z1 and Z5. Expression is more intense in
403 the wing pads, and the pattern appears to be determined by the hormonal environment:
404 maximum BR-C mRNA levels coincide with bursts of 20E production in the presence
405 of high levels of JH. The coincidence of BR-C expression peaks and those of 20E
406 reflects cause-effect relationships, as expression of BR-C is 20E-dependent [41]. Then,
407 BR-C mRNA levels decline in the last nymphal instar (N6), in parallel to JH vanishing,
408 although a small burst of expression is still observed on day 6 coinciding with a peak of
409 20E. The correspondence of BR-C and JH patterns, the induction of BR-C expression
410 by exogenous JH III, and their down-regulation after depletion of Kr-h1, suggest that JH
411 enhances BR-C expression during young nymphal instars. Therefore, the steady decline
412 observed in N6 must be due, at least in part, to the decrease of JH titer. In the
413 hemipteran *P. apterus*, treatment with a JH analogue induces ectopic expression of BR-
414 C in last nymphal instar, whereas depletion of Met expression led to a significant
415 reduction of BR-C expression [12]. These observations are in agreement with our

416 present results as Met is an early transducer of the JH signal and seems to play a role in
417 JH reception [9], also in *B. germanica* (our unpublished results).

418 Significant expression of BR-C in young nymphal instars has been reported in
419 the hemimetabolous species *O. fasciatus* [29] and *P. apterus* [12]. Conversely, BR-C
420 expression in holometabolous species is quantitatively relevant only in the larva-pupa
421 transition. This includes *D. melanogaster* [25], *M. sexta* [25], *B. mori* [42] and *T.*
422 *castaneum* [11, 27, 28]. Data from holometabolous species suggest that the onset of BR-
423 C expression occurs after a small burst of 20E produced in the absence of JH at the end
424 of the last larval instar. In *M. sexta*, BR-C transcripts appear at the end of the feeding
425 stage (beginning of wandering behavior) in the epidermis of last instar larvae, when the
426 insect becomes committed to pupal differentiation. Administration of JH in this stage
427 prevents the 20E-induced expression of BR-C [43]. Later, levels of BR-C mRNA
428 decrease during the pupal stage and the pupae transform into the adult stage. In pupae,
429 exogenous JH induces the re-expression of BR-C, and the insect undergoes a second
430 pupal molt [25].

431 The expression patterns of BR-C isoforms in the thysanopterans *Frankliniella*
432 *occidentalis* and *Haplothrips brevitubus* [44], are especially interesting. Thysanopterans
433 follow an essentially hemimetabolous development, in the sense that nymphs are
434 morphologically similar to adults, but the life cycle includes 1 to 3 quiescent stages,
435 called propupae and pupae, where wing buds develop considerably and which are
436 reminiscent of the holometabolous pupal stage. This particular cycle has been
437 distinguished as neometabolism development [5]. *F. occidentalis* has two nymphal
438 stages, a propupal and a pupal stage, whereas *H. brevitubus* has two nymphal stages, a
439 propupal and two pupal stages. In both species, expression of BR-C is low in the first
440 instar nymph, peaks towards the end of the second instar nymph and decreases in the
441 propupae. Moreover, treatment of propupae with a JH analog induces the re-expression
442 of BR-C in the pupae [44]. The BR-C expression pattern, showing a peak just before the
443 transition from nymph to propupae, and the stimulatory effect of JH on BR-C
444 expression in the propupae, are reminiscent of the endocrine determinism of the pupal
445 stage in holometabolous species.

446

447 *4.2. The functions*

448 RNAi experiments in nymphs of *B. germanica* have shown that wing buds
449 experience intense cell proliferation, which is hampered in BR-C knockdowns. This
450 suggests that BR-C isoforms regulate progressive growth of wing buds during nymphal
451 life by promoting cell division. In the last nymphal instar there is a phase of cell
452 proliferation encompassed by the increasing levels of 20E that lead to the peak on day 6,
453 followed by a phase of cell growth and wing metamorphosis encompassed by the
454 decreasing levels of 20E that occur after the peak. In this metamorphic instar, cell
455 proliferation is also hampered in BR-C knockdowns, but the subsequent phase of cell
456 growth and metamorphosis is generally not affected by BR-C RNAi. Only some details
457 of vein patterning in the hindwing are affected by BR-C RNAi, including the length of
458 the CuP vein, the organization of the longitudinal and small transversal veins in the
459 anterior part of the hindwing, and the linear growth of the A-veins in the posterior part.

460 Therefore, the function of BR-C isoforms in postembryonic development of *B.*
461 *germanica* appears to be restricted to sustaining cell division in the wing buds, which
462 contributes to the final size and morphology of the adult wings, and regulation of a
463 number of details of vein patterning and length and in the hindwing. While the latter
464 function had not been described before in hemimetabolous insects, our observations on
465 wing size are equivalent to those obtained in *O. fasciatus* and *P. apterus*, where RNAi
466 treatments of BR-C hampered wing bud development in nymphs and resulted in adults
467 with reduced and wrinkled wings [12, 29]. Our observations refer to the external
468 morphology, as no anatomical examinations were carried out during the present work.
469 Thus, we cannot rule out the possibility of a possible role of BR-C factors in the
470 nervous system during metamorphosis of *B. germanica*, as occurs in *D. melanogaster*
471 [45, 46]. However, the primitive hemimetaboly exhibited by *B. germanica* suggests that
472 there are no dramatic transformations of the internal organs, as opposed to *D.*
473 *melanogaster*, whose internal anatomy is heavily reconstructed during metamorphosis.

474 In striking contrast, BR-C proteins play complex morphogenetic roles in
475 holometabolous species, leading to the formation of the pupal morphology. Pioneering
476 genetic studies in *D. melanogaster* demonstrated that BR-C null mutants, in which not
477 one of the isoforms is expressed, never molt to pupae [23, 47, 48]. Later, the use of a
478 recombinant Sindbis virus expressing a BR-C antisense RNA fragment in *B. mori*,
479 reduced endogenous BR-C mRNA levels in infected tissues and the insect did not
480 complete the larval-pupal transition [26]. More recently, experiments depleting BR-C

481 mRNA levels with RNAi have been carried out in *T. castaneum* [11, 27, 28] and in the
482 lacewing *Chrysopa perla* [28]. In all cases, RNAi treatments in larvae hampered larval-
483 pupal transformation and produced individuals with larval, pupal and adult features,
484 which indicates that BR-C isoforms promote the pupal developmental program while
485 suppressing those of the larvae and the adult.

486

487 4.3. The isoforms

488 In *D. melanogaster*, BR-C encodes four zinc-finger protein isoforms (Z1, Z2, Z3
489 and Z4), which share most of the amino-terminal region called the BRcore, but they
490 have a unique pair of zinc-fingers at their carboxy terminus [23, 24]. Moreover, the
491 common BRcore region contains a BR-C-Tramtrack-Bric-à-brac (BTB) domain
492 involved in protein-protein interactions [24]. Mutants corresponding to isoform-specific
493 regions form three complementing groups: *br* (*broad*), *rbp* (*reduced bristle number on*
494 *palpus*) and *2Bc* [47, 48]. Alleles belonging to the *npr1* (*nonpupariating1*) class of
495 mutations does not complement mutations in each of the three complementing genetic
496 functions. *npr1* mutations result in developmental arrest and lethality at pupariation; *br*⁺
497 function is required for wing and leg imaginal disc development and for tanning the
498 larval cuticle; *rbp*⁺ and *2Bc*⁺ functions are needed for larval tissues destruction and for
499 gut morphogenesis; moreover, *2Bc*⁺ is additionally required for complete closure of the
500 thoracic epidermis, and all three functions must occur for central nervous system
501 reorganization [47-50]. Mutant rescue experiments associated protein isoforms with
502 genetic functions, and revealed that there were isoform-specific functions, although with
503 some degree of redundancy [51]. Further studies in *D. melanogaster* have shown
504 specific space-temporal distributions of different BR-C isoforms, thus suggesting
505 distinct temporal function, especially in neural tissue morphogenesis [45, 46, 52].
506 Finally, the advent of RNAi allowed the functional study of individual BR-C isoforms
507 (Z1 to Z5) in *T. castaneum* metamorphosis. As in *D. melanogaster*, results pointed to
508 isoform-specific roles and partial redundancy [27, 28].

509 Our functional studies on specific isoforms revealed that depletion of BR-C Z2
510 and BR-C Z6 gave discernible phenotypes, in both cases related to wing patterning. BR-
511 C Z2 phenotype showed the CuP vein shorter and an associated notch at the wing edge
512 (defect A), and the vein/intervein patterning disorganized in the anterior part (defect B),
513 but it did not show the A-veins subdivided and incomplete (defect C). Moreover, the

514 penetrance and severity of the defects were lower in comparison with the BR-C Core
515 knockdowns, whilst wing size was practically unaffected. BR-C Z6 knockdowns
516 phenotype showed t defects B and C, but not defect A, which is the most typical in the
517 experiments depleting all isoforms simultaneously; wing size was unaffected.
518 Phenotypes obtained in RNAi experiments on BR-C Z1, BR-C Z3, BR-C Z4 and BR-C
519 Z5 were as in controls, including defect B, which seems qualitatively unspecific,
520 although, importantly, its occurrence in BRCore or BR-C Z6 knockdowns is
521 significantly higher than in controls. The relatively poor abundance of these isoforms in
522 the pool of BR-C proteins, and the generally modest efficiency of these RNAi
523 experiments in terms of transcript decrease, might explain the absence of differential
524 phenotypes. However, given that phenotypes observed in BR-C Z2 and BR-C Z6
525 knockdowns encompass all the defects observed in BRCore knockdowns, we can
526 presume that functions of the remaining isoforms might be redundant with those of BR-
527 C Z2 and BR-C Z6.

528

529 *4.4.Conclusion: The evolution of metamorphosis at the light of BR-C*

530 The main function played by BR-C proteins in *B. germanica*, a phylogenetically
531 basal, hemimetabolous species, during post-embryogenesis is to promote wing growth
532 to reach the right size and form. Basically, this function has been conserved in the
533 hemimetabolous species *O. fasciatus* and *P. apterus*, which are phylogenetically more
534 distal than *B. germanica*. In these bugs, the wing buds are external, not embedded in a
535 cuticular wing pad pocket, and the decrease in growth and attenuation of color pattern
536 progression of BR-C knockdowns is externally visible [12, 29]. In the beetle *T.*
537 *castaneum*, RNAi of BR-C isoforms Z2 and Z3 results in pupae with shortened wings
538 [27], which indicates that functions of BR-C related to wing size are conserved in basal
539 holometabolous species. Functions of BR-C in determining wing size and form also
540 appear to be present in the extremely modified, holometabolous species of fly *D.*
541 *melanogaster*. Indeed, the name “broad” given to one of the complementation groups of
542 BR-C derives from the oval, rather than elliptic form of the wings of these mutants,
543 which were first described by Thomas H. Morgan and colleagues in 1925 [53].
544 Therefore, the functions of BR related to controlling wing size and form appear to be
545 ancestral and conserved from cockroaches to flies. The same may hold true for the
546 subtle functions related to vein patterning observed in *B. germanica*, as the classical *br*

547 mutants of *D. melanogaster* also have defects on vein length [53]. Vein patterning in
548 BR-C knockdowns of *O. fasciatus* and *P. apterus* was not reported [12, 29].

549 Another interesting feature of BR-C in *B. germanica* is that its expression is
550 enhanced by JH. Thus, both JH and BR-C mRNA levels are high in young nymphal
551 instars and decrease in parallel during the last nymphal instar, prior to metamorphosis.
552 This contrasts with the situation found in holometabolous species, where JH inhibits
553 BR-C expression in young larvae, and so high levels of JH correlate with low levels of
554 BR-C expression [12].

555 A number of theories have been proposed to explain the evolutionary transition
556 from hemimetaboly to holometaboly [4, 54]. A classic theory originally argued by
557 Lubbock [55] and formalized by Berlese [56], proposes that the larvae of
558 holometabolous species arose by “de-embryonization”, so that it was a sort of free
559 living, often vermiform embryo. The “de-embryonization” theory was resuscitated and
560 reinforced with modern endocrine data by Truman and Riddiford [54], who proposed
561 that the holometabolous larva corresponds to the latest hemimetabolous embryonic
562 stage that the latter authors called the pronymph, and that the origin of larval form
563 would be explained by a shift in JH titers, from late embryonic stages in
564 hemimetabolous species to earlier stages in holometabolous insect embryos. Thus, in
565 postembryonic stages of holometabolous species, only when JH declines in the final
566 larval instar does extensive morphogenesis resume and lead to differentiation of the
567 pupa [57].

568 While this theory still is under debate [4], our present results show that, in a
569 basal hemimetabolous species, JH enhances the expression of BR-C in young nymphs
570 and that BR-C factors promote wing growth during nymphal life and refine wing
571 patterning at metamorphosis, which contrasts with the endocrine regulation and
572 complex functions observed in holometabolous species, as previously described in
573 classical insect models. We propose that in the evolution from hemimetaboly to
574 holometaboly, at least two key innovations appeared that affected BR-C and post-
575 embryonic morphological development. The first was a shift of JH action, from
576 stimulatory (as in present hemimetabolous species) to inhibitory (present
577 holometabolous species) of BR-C expression, during young stages. Thus, BR-C
578 expression had become inhibited during young larvae in holometabolous ancestors, with
579 the resulting suppression of growth and development of BR-C-dependent tissues, for

580 example the wing bud. The second great innovation was an expansion of functions,
581 from one specialized in wing development and details of vein patterning, as in present
582 hemimetabolous species, to a larger array of morphogenetic functions, which
583 culminated with the pupal-specifier role that operates in present holometabolous
584 species, from the basal *T. castaneum* to the distal *D. melanogaster* (Fig. 5).
585 Paradoxically, the number of isoforms decreased from six to four in the evolution from
586 cockroaches to flies, while their functions dramatically expanded.

587 The case of thysanopterans is very interesting because they show the so-called
588 neometabolous development [5], with a life cycle including quiescent “propupal” and
589 “pupal” stages that are reminiscent of the holometabolous pupae. The studies in *F.*
590 *occidentalis* and *H. brevitubus* of Minakuchi et al. [44] have shown that BR-C mRNA
591 levels are very low in young instars and show an acute peak around the formation of the
592 propupae, as occurs in holometabolous species, suggesting that BR-C expression in
593 thysanopterans is hormonally regulated and specified as in holometabolous species.
594 Reconstructions of insect phylogeny suggest that paraneopterans ((thysanopterans +
595 hemipterans)+(psocopterans and phthirapterans)) are the sister group of Holometabola
596 [58]. If so, then the first steps toward the innovation of the pupal stage, including the
597 endocrine determination, might have occurred in the ancestor of Paraneoptera +
598 Holometabola. Interestingly, hemipterans also contain representatives of neometabolous
599 development in the Sternorrhyncha [4, 5]. Our hypothesis contemplates that other
600 Hemipterans, and Psocopterans and Phthirapterans would have lost the ability to
601 produce preimaginal quiescent stages in their life cycles. Whichever the case, although
602 natural selection was able to make a first attempt to invent a sort of pupa in the ancestor
603 of the Paraneoptera + Holometabola, the invention was fully perfected in the lineage of
604 Holometabola judging by the endless forms most beautiful that stand today in this insect
605 superorder.

606

607 **Acknowledgement**

608 Financial support for this research was provided by the Spanish MICINN (grant
609 CGL2008-03517/BOS to X.B. and predoctoral fellowship to J.L.) and by the CSIC
610 (grant 2010TW0019, from the Formosa program, to X.B.). J.-H.H received a grant from
611 the National Research Council (Taiwan) to work in the Institute of Evolutionary
612 Biology, in Barcelona. Thanks are also due to Maria-Dolors Piulachs for helpful

613 discussions, and to José Martínez for helping in the experimental work.

614

615 **Appendix A. Supplementary data**

616 Supplementary data to this article can be found online at doi: XXX

617

618

619 **Figure legends**

620

621 **Fig. 1.** Expression of BR-C mRNA in *Blattella germanica* female. (A) Joint expression
622 of all isoforms in the whole body in selected days of the 6 nymphal instars: N1 to N6.
623 (B) Joint expression of all isoforms in the mesonotum and metanotum wing pads in
624 selected days of N4, N5 and N6. Concentration patterns of hemolymph juvenile
625 hormone (JH) III and 20-hydroxyecdysone (20E) are indicated below, according to
626 previously published data [33, 40]. (C) Expression of individual BR-C isoforms (Z1 to
627 Z6) in the wing pads on selected days of N6. (D) Effect of the application of 20 µg of
628 JH III. The hormone was administered on freshly emerged N6 and BR-C mRNA levels
629 were measured 2, 4 and 6 days later. (E) Effect of Kr-h1 depletion by RNAi on N4 and
630 N5. Two doses (3 µg each) of dsKr-h1 (treated) or dsMock (control) were administered
631 on N4 and N5 (on days 0 and 3 in both cases), and BR-C mRNA levels were measured
632 on day 4 in the experiments of N4, and on day 6 in the experiments of N5. Data is
633 represented as the mean ± SEM, and are indicated as copies of BR-C mRNA per 1,000
634 copies of BgActin-5c. Each point represents 3-6 biological replicates, except in panel C,
635 in which data represent one replicate per point. In panels D and E data are normalized
636 against control females (arbitrary reference value = 1) and the asterisk indicates
637 statistically significant differences with respect to controls ($p < 0.05$), according to the
638 REST software tool [31].

639

640 **Fig. 2.** Phenotype obtained after depleting all BR-C isoforms by RNAi in *Blattella*
641 *germanica*. (A-B) Effect of a single 3 µg-dose of dsMock (control) or dsBR-core
642 (treated) administered on day 0 of N5: BR-C mRNA levels on day 6 of N5 and on day 0
643 of N6 (A); adult phenotype (habitus, forewing and hindwing) (B). (C-D) Effects of two
644 doses of 3 µg each of dsBR-core administered on day 0 and day 3 of N5: BR-C mRNA
645 levels on day 0 of N6 (C); extended wings and wrinkled wings phenotype (D). (E-F)
646 Effects of two 3 µg-doses of dsBR-core administered on day 0 and day 3 of N4: BR-C
647 mRNA levels on day 0 of N5 (E); extended wings and wrinkled wings phenotype (F).
648 (G-H) Effects of two 3 µg-doses of dsMock (control) or dsBR-core (treated)
649 administered on day 0 and day 3 of N6: BR-C mRNA levels on day 6 of N6 (G); adult
650 phenotype of controls and treated specimens (H). Data in (A), (C), (E) and (G) represent

651 3 biological replicates (mean \pm SEM), are indicated as copies of BR-C mRNA per 1,000
652 copies of BgActin-5c, and are normalized against control females (arbitrary reference
653 value = 1); the asterisk indicates statistically significant differences with respect to
654 controls ($p < 0.05$), according to the REST software tool [31]. Arrows indicate the notch
655 provoked by a shortening of the CuP vein, and the arrowhead indicates disorganized
656 vein/intervein patterning in the anterior part of the hindwing. Note that the late defect
657 appeared also in controls (H).

658

659 **Fig. 3.** Development of wing buds in control and BR-C knockdown specimens of
660 *Blattella germanica*. (A) Double labeling EdU (discrete red spots) and DAPI (blue
661 color) of a hindwing bud of untreated females on days 5, 6 and 7 of the last nymphal
662 instar (N6). (B) EdU-DAPI double labeling of a forewing bud of females that were
663 treated with two doses of dsBrCore (treated) or of dsMock (control) administered on
664 days 0 and 3 of N5, and photographed on days 5 and 6 of N6. (C) EdU-DAPI double
665 labeling of a hindwing bud of females that were treated as in (B) and photographed on
666 day 5 of N6; the pictures show the region corresponding to the distal end of the CuP
667 vein (yellow oval).

668

669 **Fig. 4.** Effects obtained after depleting each BR-C isoform, from Z1 to Z6, individually,
670 by RNAi in *Blattella germanica*. (A-F) Transcript levels of the targeted and the other
671 isoforms measured in the mesonotum and metanotum wing pads on the day 0 of N6.
672 Two 3- μ g doses of dsBrZ2 (A), dsBrZ3 (B), dsBrZ6 (C), dsBrZ4 (D), dsBrZ1 (E) or
673 dsBrZ5 (F) administered on days 0 and 3 of N5; control received an equivalent
674 treatment with dsMock; data represent 3 biological replicates (mean \pm SEM) and are
675 indicated as copies of the individual BR-C isoforms mRNA per 1,000 copies of
676 BgActin-5c; the asterisk indicates statistically significant differences with respect to
677 controls ($p < 0.05$), according to the REST software tool [31]. (G-I) Adult hindwing
678 phenotype studied 3 days after the imaginal molt, from a dsBrZ2-treated specimen (G),
679 a dsBrZ6-treated specimen (H), and from a control specimen treated with dsMock. The
680 arrow indicates the main defects: the notch at the end of the CuP vein in G and the vein
681 pattern disorganized in the anterior part of the wing in H.

682

683 **Fig. 5.** BR-C and the evolution of insect metamorphosis. In the transition from
684 hemimetaboly to holometaboly, the regulation and functions of BR-C would have
685 experienced two main changes. First, a shift of JH action on BR-C expression, from
686 stimulatory in hemimetabolous to inhibitory in holometabolous species. Second, an
687 expansion of functions, from controlling wing pad growth by cell proliferation along
688 nymphal instars, and regulating subtle features of vein development and patterning
689 (hemimetabolous), to regulating pupal formation and inhibiting adult features at the end
690 of the larval life (holometabolous).
691

692 **References**

- 693 [1] C. Darwin, The origin of species by means of natural selection, or the
694 preservation of favoured races in the struggle for life, John Murray, London, 1872.
- 695 [2] D. Grimaldi, M.S. Engel, Evolution of the insects, Cambridge University Press,
696 Cambridge, 2005.
- 697 [3] P. Hammond, Species inventory, in: B. Groombridge (Ed.) Global biodiversity,
698 Chapman and Hall, London, 1992, pp. 17-39.
- 699 [4] X. Belles, Origin and Evolution of Insect Metamorphosis, in: Encyclopedia of
700 Life Sciences, John Wiley and Sons, Ltd., Chichester, 2011.
- 701 [5] F. Sehnal, P. Svacha, J. Zrzavy, Evolution of insect metamorphosis, in: L.I.
702 Gilbert, J.R. Tata, B.G. Atkinson (Eds.) Metamorphosis, Academic Press, San Diego,
703 1996, pp. 3-58.
- 704 [6] J.W. Truman, L.M. Riddiford, Endocrine insights into the evolution of
705 metamorphosis in insects, Annu. Rev. Entomol. 47 (2002) 467-500.
- 706 [7] L.M. Riddiford, How does juvenile hormone control insect metamorphosis and
707 reproduction?, Gen. Comp. Endocrinol. (2012) (in press).
- 708 [8] M. Jindra, S.R. Palli, L.M. Riddiford, The Juvenile Hormone Signaling Pathway
709 in Insect Development, Annu. Rev. Entomol. (2012) (in press).
- 710 [9] J.P. Charles, T. Iwema, V.C. Epa, K. Takaki, J. Rynes, M. Jindra, Ligand-binding
711 properties of a juvenile hormone receptor, Methoprene-tolerant, Proc. Natl. Acad. Sci.
712 U.S.A. 108 (2011) 21128-21133.
- 713 [10] B. Konopova, M. Jindra, Juvenile hormone resistance gene Methoprene-tolerant
714 controls entry into metamorphosis in the beetle *Tribolium castaneum*, Proc. Natl. Acad.
715 Sci. U.S.A. 104 (2007) 10488-10493.
- 716 [11] R. Parthasarathy, A. Tan, H. Bai, S.R. Palli, Transcription factor broad
717 suppresses precocious development of adult structures during larval-pupal
718 metamorphosis in the red flour beetle, *Tribolium castaneum*, Mech. Dev. 125 (2008)
719 299-313.
- 720 [12] B. Konopova, V. Smykal, M. Jindra, Common and distinct roles of juvenile
721 hormone signaling genes in metamorphosis of holometabolous and hemimetabolous
722 insects, PloS One 6 (2011) e28728.
- 723 [13] C. Minakuchi, X. Zhou, L.M. Riddiford, Kruppel homolog 1 (Kr-h1) mediates
724 juvenile hormone action during metamorphosis of *Drosophila melanogaster*, Mech.
725 Dev. 125 (2008) 91-105.
- 726 [14] C. Minakuchi, T. Namiki, T. Shinoda, Kruppel homolog 1, an early juvenile
727 hormone-response gene downstream of Methoprene-tolerant, mediates its anti-
728 metamorphic action in the red flour beetle *Tribolium castaneum*, Dev. Biol. 325 (2009)
729 341-350.
- 730 [15] J. Lozano, X. Belles, Conserved repressive function of Kruppel homolog 1 on
731 insect metamorphosis in hemimetabolous and holometabolous species, Sci. Rep. 1
732 (2011) 163.
- 733 [16] K. King-Jones, C.S. Thummel, Nuclear receptors--a perspective from
734 *Drosophila*, Nat. Rev. Genet. 6 (2005) 311-323.

- 735 [17] Y. Nakagawa, V.C. Henrich, Arthropod nuclear receptors and their role in
736 molting, *FEBS J.* 276 (2009) 6128-6157.
- 737 [18] C.S. Thummel, Ecdysone-regulated puff genes 2000, *Insect Biochem. Mol. Biol.*
738 32 (2002) 113-120.
- 739 [19] V.P. Yin, C.S. Thummel, Mechanisms of steroid-triggered programmed cell
740 death in *Drosophila*, *Semin. Cell Dev. Biol.* 16 (2005) 237-243.
- 741 [20] J. Cruz, C. Nieva, D. Mane-Padros, D. Martin, X. Belles, Nuclear receptor
742 BgFTZ-F1 regulates molting and the timing of ecdysteroid production during nymphal
743 development in the hemimetabolous insect *Blattella germanica*, *Dev. Dyn.* 237 (2008)
744 3179-3191.
- 745 [21] D. Mane-Padros, F. Borrás-Castells, X. Belles, D. Martin, Nuclear receptor HR4
746 plays an essential role in the ecdysteroid-triggered gene cascade in the development of
747 the hemimetabolous insect *Blattella germanica*, *Mol. Cell Endocrinol.* 348 (2012) 322-
748 330.
- 749 [22] D. Martin, O. Maestro, J. Cruz, D. Mane-Padros, X. Belles, RNAi studies reveal
750 a conserved role for RXR in molting in the cockroach *Blattella germanica*, *J. Insect*
751 *Physiol.* 52 (2006) 410-416.
- 752 [23] C.A. Bayer, B. Holley, J.W. Fristrom, A switch in broad-complex zinc-finger
753 isoform expression is regulated posttranscriptionally during the metamorphosis of
754 *Drosophila* imaginal discs, *Dev. Biol.* 177 (1996) 1-14.
- 755 [24] P.R. DiBello, D.A. Withers, C.A. Bayer, J.W. Fristrom, G.M. Guild, The
756 *Drosophila* Broad-Complex encodes a family of related proteins containing zinc fingers,
757 *Genetics* 129 (1991) 385-397.
- 758 [25] X. Zhou, L.M. Riddiford, Broad specifies pupal development and mediates the
759 'status quo' action of juvenile hormone on the pupal-adult transformation in *Drosophila*
760 and *Manduca*, *Development* 129 (2002) 2259-2269.
- 761 [26] M. Uhlirova, B.D. Foy, B.J. Beaty, K.E. Olson, L.M. Riddiford, M. Jindra, Use
762 of Sindbis virus-mediated RNA interference to demonstrate a conserved role of Broad-
763 Complex in insect metamorphosis, *Proc. Natl. Acad. Sci. U.S.A.* 100 (2003) 15607-
764 15612.
- 765 [27] Y. Suzuki, J.W. Truman, L.M. Riddiford, The role of Broad in the development
766 of *Tribolium castaneum*: implications for the evolution of the holometabolous insect
767 pupa, *Development* 135 (2008) 569-577.
- 768 [28] B. Konopova, M. Jindra, Broad-Complex acts downstream of Met in juvenile
769 hormone signaling to coordinate primitive holometabolous metamorphosis, *Development*
770 135 (2008) 559-568.
- 771 [29] D.F. Erezyilmaz, L.M. Riddiford, J.W. Truman, The pupal specifier broad directs
772 progressive morphogenesis in a direct-developing insect, *Proc. Natl. Acad. Sci. U.S.A.*
773 103 (2006) 6925-6930.
- 774 [30] M.D. Piulachs, V. Pagone, X. Belles, Key roles of the Broad-Complex gene in
775 insect embryogenesis, *Insect Biochem. Mol. Biol.* 40 (2010) 468-475.
- 776 [31] M.W. Pfaffl, G.W. Horgan, L. Dempfle, Relative expression software tool
777 (REST) for group-wise comparison and statistical analysis of relative expression results
778 in real-time PCR, *Nucleic Acids Res.* 30 (2002) e36.

- 779 [32] F. Camps, J. Casas, F.J. Sanchez, A. Messegue, Identification of juvenile
780 hormone III in the hemolymph of *Blattella germanica* adult females by gas
781 chromatography–mass spectrometry, Arch. Insect Biochem. Physiol. 6 (1987) 181-189.
- 782 [33] K. Treiblmayr, N. Pascual, M.D. Piulachs, T. Keller, X. Belles, Juvenile hormone
783 titer versus juvenile hormone synthesis in female nymphs and adults of the German
784 cockroach, *Blattella germanica*, J. Insect Sci. 6 (2006) 47.
- 785 [34] E. Gomez-Orte, X. Belles, MicroRNA-dependent metamorphosis in
786 hemimetabolous insects, Proc. Natl. Acad. Sci. U.S.A. 106 (2009) 21678-21682.
- 787 [35] X. Belles, Beyond *Drosophila*: RNAi in vivo and functional genomics in insects,
788 Annu. Rev. Entomol. 55 (2010) 111-128.
- 789 [36] L. Ciudad, M.D. Piulachs, X. Belles, Systemic RNAi of the cockroach
790 vitellogenin receptor results in a phenotype similar to that of the *Drosophila* yolkless
791 mutant, FEBS J. 273 (2006) 325-335.
- 792 [37] J.L. Maestro, X. Belles, Silencing allatostatin expression using double-stranded
793 RNA targeted to preproallatostatin mRNA in the German cockroach, Arch. Insect
794 Biochem. Physiol. 62 (2006) 73-79.
- 795 [38] A. Salic, T.J. Mitchison, A chemical method for fast and sensitive detection of
796 DNA synthesis in vivo, Proc. Natl. Acad. Sci. U.S.A. 105 (2008) 2415-2420.
- 797 [39] M.W. Pfaffl, G.W. Horgan, L. Dempfle, Relative expression software tool
798 (REST) for group-wise comparison and statistical analysis of relative expression results
799 in real-time PCR, Nucleic Acids Res. 30 (2002) e36.
- 800 [40] I. Romaña, N. Pascual, X. Bellés, The ovary is a source of circulating
801 ecdysteroids in *Blattella germanica* (L.) (Dictyoptera, Blattellidae), Eur. J. Entomol. 92
802 (1995) 93-103.
- 803 [41] F.D. Karim, G.M. Guild, C.S. Thummel, The *Drosophila* Broad-Complex plays
804 a key role in controlling ecdysone-regulated gene expression at the onset of
805 metamorphosis, Development 118 (1993) 977-988.
- 806 [42] A.M. Reza, Y. Kanamori, T. Shinoda, S. Shimura, K. Mita, Y. Nakahara, M.
807 Kiuchi, M. Kamimura, Hormonal control of a metamorphosis-specific transcriptional
808 factor Broad-Complex in silkworm, Comp. Biochem. Physiol. B Biochem. Mol. Biol.
809 139 (2004) 753-761.
- 810 [43] B. Zhou, K. Hiruma, T. Shinoda, L.M. Riddiford, Juvenile hormone prevents
811 ecdysteroid-induced expression of broad complex RNAs in the epidermis of the tobacco
812 hornworm, *Manduca sexta*, Dev. Biol. 203 (1998) 233-244.
- 813 [44] C. Minakuchi, M. Tanaka, K. Miura, T. Tanaka, Developmental profile and
814 hormonal regulation of the transcription factors broad and Kruppel homolog 1 in
815 hemimetabolous thrips, Insect Biochem. Mol. Biol. 41 (2011) 125-134.
- 816 [45] R.F. Spokony, L.L. Restifo, Broad Complex isoforms have unique distributions
817 during central nervous system metamorphosis in *Drosophila melanogaster*, J. Comp.
818 Neurol. 517 (2009) 15-36.
- 819 [46] B. Zhou, D.W. Williams, J. Altman, L.M. Riddiford, J.W. Truman, Temporal
820 patterns of broad isoform expression during the development of neuronal lineages in
821 *Drosophila*, Neural Dev. 4 (2009) 39.
- 822 [47] E.S. Belyaeva, M.G. Aizenzon, V.F. Semeshin, Kiss, II, K. Koczka, E.M.

823 Baritcheva, T.D. Gorelova, I.F. Zhimulev, Cytogenetic analysis of the 2B3-4--2B11
824 region of the X-chromosome of *Drosophila melanogaster*. I. Cytology of the region and
825 mutant complementation groups, *Chromosoma* 81 (1980) 281-306.

826 [48] I. Kiss, A.H. Beaton, J. Tardiff, D. Fristrom, J.W. Fristrom, Interactions and
827 developmental effects of mutations in the Broad-Complex of *Drosophila melanogaster*,
828 *Genetics* 118 (1988) 247-259.

829 [49] J.C. Fletcher, C.S. Thummel, The ecdysone-inducible Broad-complex and E74
830 early genes interact to regulate target gene transcription and *Drosophila* metamorphosis,
831 *Genetics* 141 (1995) 1025-1035.

832 [50] L.L. Restifo, K. White, Mutations in a steroid hormone-regulated gene disrupt
833 the metamorphosis of the central nervous system in *Drosophila*, *Dev. Biol.* 148 (1991)
834 174-194.

835 [51] C.A. Bayer, L. von Kalm, J.W. Fristrom, Relationships between protein isoforms
836 and genetic functions demonstrate functional redundancy at the Broad-Complex during
837 *Drosophila* metamorphosis, *Dev. Biol.* 187 (1997) 267-282.

838 [52] R.F. Spokony, L.L. Restifo, Anciently duplicated Broad Complex exons have
839 distinct temporal functions during tissue morphogenesis, *Dev. Genes Evol.* 217 (2007)
840 499-513.

841 [53] T.H. Morgan, C. Bridges, A.H. Sturtevant, The genetics of *Drosophila*, *Bibliogr.*
842 *Genet.* 2 (1925) 145.

843 [54] J.W. Truman, L.M. Riddiford, The origins of insect metamorphosis, *Nature* 401
844 (1999) 447-452.

845 [55] J. Lubbock, On the origin and metamorphoses of insects, Macmillan and Co. ,
846 London, 1895.

847 [56] A. Berlese, Intorno alle metamorfosi degli insetti, *Redia* 9 (1913) 121-136.

848 [57] J.W. Truman, L.M. Riddiford, The morphostatic actions of juvenile hormone,
849 *Insect Biochem. Mol. Biol.* 37 (2007) 761-770.

850 [58] W.C. Wheeler, M. Whiting, Q.D. Wheeler, J.M. Carpenter, The phylogeny of the
851 extant hexapod orders, *Cladistics* 17 (2001) 113-169.

852

853

854

1 *Broad-complex* functions in postembryonic development of the cockroach *Blattella*
2 *germanica* shed new light on the evolution of insect metamorphosis

3

4 Jia-Hsin Huang ^{a, b} Jesus Lozano ^a and Xavier Belles ^{a, *}

5

6 ^a Institute of Evolutionary Biology (CSIC-Universitat Pompeu Fabra), Passeig Marítim
7 de la Barceloneta 37, 08003 Barcelona, Spain

8 ^b Permanent address: Department of Entomology, National Taiwan University, Taipei
9 106, Taiwan

10

11

12 * Corresponding author at: Institute of Evolutionary Biology (CSIC-UPF), Passeig
13 Marítim de la Barceloneta 37, 08003 Barcelona, Spain. Tel.: +34 932309636; fax: +34
14 932211011. E-mail address: xavier.belles@ibe.upf-csic.es (X. Belles).

15

16 *Key Words:*

17 Insect metamorphosis

18 juvenile hormone

19 ecdysone

20 evolution of holometaboly

21 *Drosophila*

22 *Tribolium*

23 cockroach

24

25 ABSTRACT

26 *Background:* Insect metamorphosis proceeds in two modes: hemimetaboly, gradual
27 change along the life cycle, and holometaboly, abrupt change from larvae to adult
28 mediated by a pupal stage. Both are regulated by 20-hydroxyecdysone (20E), which
29 promotes molts, and juvenile hormone (JH), which represses adult morphogenesis.
30 Expression of Broad complex (BR-C) is induced by 20E and modulated by JH. In
31 holometabolous species, like *Drosophila melanogaster*, BR-C expression is inhibited by
32 JH in young larvae and enhanced in mature larvae, when JH declines and BR-C
33 expression specifies the pupal stage.

34 *Methods:* Using *Blattella germanica* as a basal hemimetabolous model, we determined
35 the patterns of expression of BR-C mRNAs using quantitative RT-PCR, and we studied
36 the functions of BR-C factors using RNA interference approaches.

37 *Results:* We found that BR-C expression is enhanced by JH and correlates with JH
38 hemolymph concentration. BR-C factors appear involved in cell division and wing pad
39 growth, as well as wing vein patterning.

40 *Conclusions:* In *B. germanica*, expression of BR-C is enhanced by JH, and BR-C
41 factors appear to promote wing growth to reach the right size, form and patterning,
42 which contrast with the endocrine regulation and complex functions observed in
43 holometabolous species.

44 *General significance:* Our results sheds new light to the evolution from hemimetaboly
45 to holometaboly regarding BR-C, whose regulation and functions were affected by two
46 innovations: 1) a shift in JH action on BR-C expression during young stages, from
47 stimulatory to inhibitory, and 2) an expansion of functions, from regulating wing
48 development, to determining pupal morphogenesis.

49

50 **1. Introduction**

51 The origin and evolution of insect metamorphosis poses one of the most
52 enigmatic conundrums in evolutionary biology. In his “On the Origin of Species”,
53 Charles Darwin already complained about the difficulty of integrating insect
54 metamorphosis (due to the striking difference between the morphologies and life styles
55 of larvae and adults of the same species) into his theory of species evolution by natural
56 selection [1]. However, it is clear that insect metamorphosis has been a key innovation
57 in insect evolution as most of the present biodiversity on Earth is composed of
58 metamorphosing insects, with approximately 1 million species described, and 10-30
59 million still to be discovered [2, 3].

60 The first systematic studies on insect metamorphosis were carried out by
61 Renaissance entomologists, who established that post-embryonic changes are most
62 spectacular in insects like butterflies, beetles and flies, which undergo a dramatic
63 morphological transformation from larva to pupa and adult, a phenomenon now known
64 as holometaboly. Other insects, such as locusts and cockroaches, also metamorphose
65 from the last nymphal instar to adult, although the change of form is not as radical given
66 that the nymphs are similar to the adults. However, they undergo qualitative
67 metamorphic changes, such as formation of mature wings and external genitalia in a
68 type of metamorphosis known as hemimetaboly [4, 5]. Metamorphosis evolved from
69 hemimetaboly to holometaboly, and the latter innovation was most successful because
70 more than 80% of present insects are holometabolous species (including the “big four”
71 orders: Lepidoptera, Coleoptera, Diptera and Hymenoptera) [2, 3]. Therefore,
72 explaining the evolutionary transition from hemimetaboly to holometaboly may give a
73 new look to explain how this amazing biodiversity originated, and the study of the
74 processes regulating metamorphosis shall surely provide important clues for such a goal
75 [6].

76 Insect metamorphosis is regulated by two hormones, the molting hormone,
77 which promotes molting, and the juvenile hormone (JH), which represses
78 metamorphosis and, thus determines the molt type: to an immature stage when it is
79 present, or to the adult when it is absent [4, 6, 7]. Although the molecular action of JH is
80 still poorly understood [8], we know that an important transducer of the JH signal is
81 Methoprene tolerant (Met), a transcription factor that was discovered in *Drosophila*
82 *melanogaster* and that plays an important role in JH reception [9]. Key functional

83 evidence that Met is required for the repressor action of JH on metamorphosis was
84 obtained from the beetle *Tribolium castaneum*, a basal holometabolous insect where
85 depletion of Met expression induced larvae to undergo precocious metamorphosis [10,
86 11]. More recently, the function of Met as an early JH transducer has been demonstrated
87 in the hemimetabolous species *Pyrrhocoris apterus* [12], which established the first
88 regularity in the signaling pathway of JH in hemimetabolous and holometabolous
89 insects. Another important element in JH transduction in relation to metamorphosis is
90 the transcription factor Krüppel homolog 1 (Kr-h1), whose antimetamorphic action was
91 firstly demonstrated in *D. melanogaster* [13] and *T. castaneum* [14]. More recently, the
92 role of Kr-h1 as a transducer of the JH signal has been reported in three
93 hemimetabolous insects: the cockroach *Blattella germanica* [15] and the bugs *P. apterus*
94 and *Rhodnius prolixus* [12]. RNAi studies in these species have shown that Kr-h1
95 represses metamorphosis and that it acts downstream of Met in the JH signaling
96 pathway. Kr-h1 therefore appears to be the more distal transcription factor in the JH
97 signaling cascade whose role as mediator of the antimetamorphic action of JH has been
98 conserved from cockroaches to flies. The next challenge is to unveil the factor(s)
99 specifying the adult stage that are repressed by Kr-h1.

100 Concerning the molecular action of molting hormones, the effect of 20-
101 hydroxyecdysone (20E) is also mediated by a cascade of transcription factors that starts
102 upon its binding to the heterodimeric receptor composed of the ecdysone receptor and
103 the ultraspiracle, which belong to the nuclear receptor superfamily. This activates
104 expression of a hierarchy of transcription factors generally belonging to the same
105 superfamily, like E75, E78, HR3, HR4 and FTZ-F1, which regulate the genes that
106 underlie the cellular changes associated to molting and metamorphosis [16, 17]. Most of
107 the information available on this cascade refers to *D. melanogaster* [18, 19], but there
108 are a good deal of data from hemimetabolous species, especially from the cockroach *B.*
109 *germanica*. Factors involved in 20E signaling in *B. germanica* are generally the same as
110 in *D. melanogaster*, although the functions of some of them and their epistatic
111 relationships may differ with respect to those observed in the fly [20-22].

112 Among the most interesting 20E-dependent factors are the products of the Broad
113 complex (BR-C) gene, whose functions may have radically diverged in hemimetabolous
114 and holometabolous species. BR-C encodes a group of C2H2 zinc-finger transcription
115 factors [23, 24] that, in holometabolous species, like the dipteran *D. melanogaster*, the

116 lepidopterans *Manduca sexta* and *Bombyx mori*, and the coleopteran *T. castaneum*, are
117 expressed in the final larval stage, and this transient expression is essential for the
118 successful formation of the pupae [11, 25-28]. Experiments carried out on the
119 hemipterans *Oncopeltus fasciatus* [29] and *P. apterus* [12], which are phylogenetically
120 distal hemimetabolous species, suggested that BR-C transcription factors only regulate
121 gradual wing bud growth. This specific role, which is radically different from the
122 morphogenetic functions involved in pupae formation in holometabolous species,
123 prompted us to undertake a detailed functional study of BR-C in *B. germanica*, a basal
124 polyneopteran insect representing a poorly modified hemimetabolous species [4]. In *B.*
125 *germanica*, the BR-C gene encodes six zinc-finger isoforms (BR-C Z1 to Z6), which
126 play important roles in embryogenesis [30]. The present work, based on functional
127 studies in post-embryonic development, reveals ancestral functions of BR-C
128 transcription factors related to cell division and of wing pad growth, as well as to wing
129 vein patterning, and provides new clues that illuminate the evolution of insect
130 metamorphosis.

131

132 **2. Materials and methods**

133 *2.1. Insects*

134 *B. germanica* specimens used in the experiments were obtained from a colony
135 reared in the dark at $30 \pm 1^\circ\text{C}$ and 60-70% r.h. They were carbon dioxide-anaesthetized
136 prior to dissections and tissue sampling.

137

138 *2.2. RNA Extraction and retrotranscription to cDNA*

139 All RNA extractions were carried out with the Gen Elute Mammalian Total RNA
140 kit (Sigma-Aldrich, Madrid, Spain). An amount of 400 ng from each RNA extraction
141 was treated with DNase (Promega, Madison, WI, USA) and reverse transcribed with
142 Superscript II reverse transcriptase (Invitrogen, Carlsbad CA, USA) and random
143 hexamers (Promega). RNA quantity and quality was estimated by spectrophotometric
144 absorption at 260 nm in a Nanodrop Spectrophotometer ND-1000® (NanoDrop
145 Technologies, Wilmington, DE, USA).

146

147 *2.3. Determination of mRNA levels with quantitative real-time PCR*

148 Quantitative real time PCR (qRT-PCR) reactions were carried out in triplicate in
149 an iQ5 Real-Time PCR Detection System (Bio-Rad Laboratories, Madrid, Spain), using
150 SYBR®Green (Power SYBR® Green PCR Master Mix; Applied Biosystems, Madrid,
151 Spain). A control without template was included in all batches. The primers used to
152 detect all isoforms simultaneously or to detect each isoform specifically are described in
153 Table S1 (see Supplementary data). The efficiency of each primer set was first validated
154 by constructing a standard curve through four serial dilutions. mRNA levels were
155 calculated relative to BgActin- 5c (Accession number AJ862721) expression using the
156 Bio-Rad iQ5 Standard Edition Optical System Software (version 2.0). The primers used
157 to quantify BgActin-5c are indicated in Table S2 (see Supplementary data). We
158 followed a method based in Ct (threshold-cycle) according to the Pfaffl mathematical
159 model [31], simplifying to $2^{\Delta\Delta Ct}$ because the calculated efficiency values for studied
160 genes and BgActin-5c amplicons were always within the range of 95 to 100%;
161 therefore, no correction for efficiency was used in further calculations. Results are given
162 as copies of mRNA per 1,000 copies of BgActin-5c mRNA.

163

164 2.4. Treatments with juvenile hormone III in vivo

165 To study the effect of JH upon BR-C expression, JH III, which is the native JH
166 of *B. germanica* [32, 33], was applied topically to freshly emerged last instar nymphs at
167 a dose of 20 µg per specimen in 1 µl of acetone. We used JH III from Sigma-Aldrich,
168 which is a mixture of isomers containing about 50% of the biologically active (10R)-JH
169 III. Thus, the active dose applied would be around 10 µg per specimen, which is an
170 efficient dose to impair metamorphosis [34]. Controls received 1 µl of acetone.

171

172 2.5. RNA interference

173 *B. germanica* is very sensitive to RNA interference (RNAi) in vivo [35].
174 Detailed procedures for dsRNA preparation and RNAi experiments were as described
175 previously [22, 36, 37]. Concerning BR-C, dsRNAs were prepared to deplete all
176 isoforms simultaneously (dsBrCore) or specific isoforms BR-C Z1 to BR-C Z6 (dsBrZ1
177 to dsBrZ6). The primers used to generate templates with PCR for transcription of these
178 dsRNAs are described in Table S3 (see Supplementary data). The fragments were
179 amplified by PCR and cloned into the pSTBlue-1 vector (Novagen, Madrid, Spain). In

180 all cases, we used a 307 bp sequence from *Autographa californica* nucleopolyhydro-
181 virus (Accession number K01149, from nucleotide 370 to 676) as control dsRNA
182 (dsMock). A volume of 1 μ l of each dsRNA solution (3 μ g/ μ l) was injected into the
183 abdomen of specimens at chosen ages and stages. Control specimens were treated with
184 the same dose and volume of dsMock. RNAi of Kr-h1 was carried out as recently
185 reported [15].

186

187 2.6. *Wing morphological studies*

188 Development of mesonotum and metanotum wing primordia or wing buds was
189 studied in 5th (N5, penultimate) and 6th (N6, last) nymphal instars. Wing buds were
190 exposed out of the dorsal cuticular layer under Ringer's saline. Then, they were fixed in
191 4% paraformaldehyde and permeabilised in PBS-0.2% tween (PBT), incubated for 20
192 min in 300 ng/ml phalloidin-Tetramethyl Rhodamine Isothiocyanate (Sigma-Aldrich) in
193 PBT, rinsed with PBS, and stained for 10 min in 1 μ g/ml DAPI in PBT. After three
194 washes with PBT, the wing buds were mounted in Mowiol 4-88 (Calbiochem), and were
195 examined by epifluorescence microscopy AxioImager.Z1 (ApoTome System, Zeiss).
196 Adult forewings (tegmina) and hindwings (membranous) were studied and
197 photographed first in the intact animal, and then dissected out, mounted on a slide with
198 Mowiol 4-88. In these cases, examinations and photographs were made with a
199 stereomicroscope Zeiss DiscoveryV8. Biometrical measurements of wing size
200 parameters were carried out with an ocular micrometer adapted to this
201 stereomicroscope.

202

203

204 2.7. *EdU experiments to measure cell proliferation in vivo*

205 EdU (5-ethynyl-2'-deoxyuridine) is a thymidine analogue recently developed for
206 labeling DNA synthesis and dividing cells in vitro [38], which is more sensitive and
207 practical than the commonly used 5-bromo-2'-deoxyuridine, BrdU. We followed an
208 approach in vivo, using used the commercial EdU compound "Click-it EdU-Alexa
209 Fluor[®] 594 azide" (Invitrogen, Molecular Probes), which was applied topically on the
210 first abdominal tergites (10 μ g in 1 μ l of DMSO) of staged nymphs. Control specimens
211 received 1 μ l of DMSO. Wing buds from treated specimens were dissected 24 h later,
212 and processed for EdU detection according to the manufacturer's protocol.

213

214 2.8. Statistics

215 In general, data are expressed as mean \pm standard error of the mean (SEM). In
216 qRT-PCR determinations, statistical analyses between groups were tested by the REST
217 2008 program (Relative Expression Software Tool V 2.0.7; Corbett Research) [39]. This
218 program makes no assumptions about the distributions, evaluating the significance of
219 the derived results by Pair-Wise Fixed Reallocation Randomization Test tool in REST
220 [39]. Statistical analyses of wing biometrical measurements were carried out with the
221 Student's *t*-test.

222

223

224 3. Results

225 3.1. Broad complex isoforms are expressed along the entire nymphal life of *B.*

226 *germanica*

227 As a first step in our work, we studied the temporal expression of BR-C during
228 the nymphal life of the cockroach *B. germanica*. Firstly, we used whole body extracts
229 and a primer set amplifying a fragment in the core region of BR-C, which is common to
230 the six BR-C isoforms. Results obtained show that BR-C transcripts are present in the
231 six nymphal instars (N1 to N6) at levels of some 100 copies per 1,000 copies of actin
232 mRNA. In the last nymphal instar (N6), BR-C mRNA levels steadily decreased until
233 becoming practically undetectable just before molting to the adult stage (Fig. 1A).

234 Given that BR-C functions in hemimetabolous insects appeared to be associated
235 to wing growth, we obtained expression patterns in the pooled wing pads, that is, the
236 lateral expansions of the mesonotum and metanotum, which contain the wing buds,
237 during the last two nymphal instars (N5 and N6). Results revealed that BR-C is highly
238 expressed in wing pads in N5, the expression levels forming a peak on day 4. In N6 the
239 expression levels are notably lower and steadily decreasing, although showing a small
240 peak of expression on day 6 (Fig. 1B). The expression peaks in N5 and N6 correspond
241 to the peaks of 20E, and the high levels of expression in N5 correlate with the presence
242 of JH, while the levels decrease in N6 when JH vanishes (Fig. 1B, *bottom*).

243 The expression of the individual isoforms, BR-C Z1 to BR-C Z6 in the wing
244 pads during N6 show the same pattern in all isoforms: high levels at emergence, then a
245 steady decrease although with a small peak of expression on day 6 (Fig. 1C). Moreover,
246 the study shows that BR-C Z2 is the most abundant isoform, followed by Z3, Z6, Z4,

247 Z1 and Z5. With the RNA extract used to study the individual isoforms (results in Fig.
248 1C) we also amplified the core region fragment as in Fig. 1A. The mRNA values
249 obtained were similar to those resulting from the sum of values of all isoforms for each
250 day (Supplementary Fig. S1), which suggests that the six BR-C isoforms known in *B.*
251 *germanica* constitute the complete functional set.

252 As stated above, the dramatic differences of BR-C expression between N5 and
253 N6 are probably due to JH, which is abundantly present in N5 and practically absent in
254 N6. This suggests that JH enhances the expression of BR-C in *B. germanica*, and that
255 the decline of BR-C mRNA levels in N6 may largely be due to the absence of JH. In
256 agreement with this, topical treatment of freshly emerged N6 with 20 μ g of JH III
257 induced the re-expression of BR-C (Fig. 1D). Congruently, depletion of Kr-h1, a
258 transcription factor involved in early JH signaling, decreases BR-C expression levels in
259 N4 and in N5 (Fig. 1E).

260

261 3.2. BR-C depletion impairs wing development

262 To study the role of BR-C, cockroaches were treated with 3 μ g dsRNA targeting
263 the core region of BR-C (dsBrCore) at day 0 of N5. Controls were equivalently treated
264 with dsMock. On day 6 of N5 and on day 0 of N6, levels of BR-C mRNA in dsBrCore-
265 treated specimens were significantly lower than those measured in controls (Fig. 2A).
266 dsBrCore-treated specimens (n = 34) molted normally to N6, but the adults emerging
267 from the subsequent molt showed a number of differences with respect to dsMock-
268 treated controls (n = 24). In dsBrCore-treated specimens, both wing pairs were well
269 extended, but the forewings appeared to be somewhat broader and the hindwings were
270 smaller than those of the controls, and showed a number of vein defects (Fig. 2B).
271 Biometrical data supported the observations regarding form and size (Supplementary
272 Fig. S2). And as to the hind wing vein patterning, 19 out of 34 specimens (56%) had the
273 CuP vein shorter and an associated notch at the wing edge (defect A, Supplementary
274 Fig. S3); four specimens (12%) showed vein/intervein pattern disorganization in the
275 anterior part of the wing (defect B, Supplementary Fig. S3); six specimens (17%)
276 showed the defects A and B; and five specimens (15%) had A and B defects and their A-
277 veins were subdivided and incomplete (defect C, Supplementary Fig. S3). In all other
278 respects, the external morphology of the adult of dsBrCore-treated specimens was
279 normal. Control (dsMock-treated) specimens developed normally patterned wings,
280 although a small percentage of the specimens (3 out of 24, 12.5%) showed the defect B

281 (Supplementary Fig. S3).

282 We then increased the RNAi effectiveness using two doses of 3 μ g of dsBrCore,
283 administered respectively on days 0 and 3 of N5. Levels of BR-C mRNA measured on
284 day 6 of N5 (Fig. 2C) were lower than those obtained with a single injection (Fig. 2A).
285 Specimens treated twice with dsBrCore (n = 23) molted normally to N6, and then to the
286 adult stage, which showed malformed wings. About 70% of the adult specimens (16 out
287 of 23) showed a phenotype similar to that obtained with a single injection of dsRNA:
288 the wings being well extended but with the typical notch produced by a shortening of
289 the CuP vein, a similar diversity of vein patterning malformations, and with broader
290 forewings and smaller hindwings than in controls (Fig. 2D, *left*). The remaining 30%
291 exhibited a wing phenotype more severe, with the forewings and hindwings heavily
292 reduced and so wrinkled (Fig. 2D, *right*) that it was difficult to extend them on a slide;
293 however, close examination indicated that all of them had the A, B and C vein defects
294 observed in the dsBrCore-treated specimens that emerged with the wings well extended.
295 Arguably, differences in severity of the effects are due to differences of penetrance and
296 intrinsic variability in these experiments. All the controls treated equivalently with two
297 doses of dsMock (n = 18) emerged with normal wings in terms of size, form and vein
298 patterning.

299 In order to assess whether BR-C could play a role on the wing development of
300 younger instars, we administered two doses (3 μ g-each) of dsBrCore on days 0 and 3
301 respectively of N4. On day 0 of N5, levels of BR-C mRNA in dsBrCore-treated
302 specimens were significantly lower than controls (dsMock-treated) (Fig. 2E). dsBrCore-
303 treated specimens (n = 22) molted normally to N5 and to N6, but when molting to the
304 adult stage they showed the wing malformations observed in the former experiments,
305 with extended and wrinkled wing phenotypes, but with a higher proportion of the latter.
306 Thus, only six out of 22 treated specimens (27%) showed the extended wing phenotype,
307 and even these had the wings imperfectly extended (Fig. 2F, *left*); moreover, the wings
308 exhibited the A, B and C defects and reduced size typical of BR-C knockdowns. The
309 remaining 16 specimens (73%) showed the more severe wrinkled wing phenotype (Fig.
310 2F, *right*). Controls (dsMock-treated, n = 21), had normal wing patterning, except three
311 specimens (14.3%) that exhibited the B defect.

312 Finally, we aimed at studying the effect of BR-C depletion in the last instar
313 nymph (N6), where the transition to the adult stage occurs. Cockroaches were treated
314 with two doses of 3 μ g each of dsBrCore, one administered on day 0 and the other on

315 day 3 of N6. Three days later (day 6), levels of BR-C mRNA were significantly lower in
316 dsBrCore-treated insects than in controls (Fig. 2G). All adults obtained after this
317 treatment (n = 24) emerged with the wings well extended, and only 5 of them (21%)
318 showed the A defect (Fig. 2H, *right*). Control (dsMock-treated) specimens (n = 23) had
319 normal wing patterning, and only one specimen (4%) had the B defect (Fig. 2H, *left*).

320

321 *3.3. BR-C depletion impairs cell division in wing buds*

322 The decrease in wing size, especially in the hindwings, suggests that there was a
323 problem of cell proliferation in dsBrCore-treated specimens. To test this possibility, we
324 first studied cell division in the hindwing buds in N6 around the peak of 20E, which
325 takes place between days 5 and 7, with maximum values on day 6 [40]. Cell division in
326 the hindwing buds, which are located within a pocket in the lateral expansions of the
327 metanotum, was labeled with EdU. On day 5, EdU labeling revealed intense cell
328 division on the surface of the hindwing bud (Fig. 3A, *day 5*). On day 6, cell division on
329 the surface practically vanished, while the wing bud started growing and folding (Fig.
330 3A, *day 6*). Towards the end of day 6 and during the whole of day 7, EdU labeling
331 disappeared and a remarkable, general wing growth took place, that provoked multiple
332 and thick folds on the hindwing surface (Fig. 3A, *day 7*). The same transition from cell
333 division to wing growth between days 5 and 7 occurs in the forewing buds (Fig. 3B,
334 *control*), which are located within the lateral expansions of the mesonotum.

335 In specimens treated with a double dose of 3 μ g of dsBrCore administered
336 respectively on days 0 and 3 of N5, EdU labeling in the forewing buds on day 5 of N6
337 was significantly reduced in comparison with controls (dsMock-treated) (Fig. 3B, *left*
338 *panels, compare control and treated*). On day 6, during the period of growth and folding
339 in controls, remarkable surface reduction was noticed along the edges of the wing pad in
340 dsBrCore-treated specimens (Fig. 3B, *right panels, compare control and treated*), which
341 parallels the statistically significant reduction on wing size measured after the imaginal
342 molt (Supplementary Fig. S2). Concerning the hindwing buds, EdU labeling on day 5
343 was also more reduced in the specimens treated with dsBrCore than in controls treated
344 with dsMock. Differences were particularly obvious at the distal end of the CuP vein,
345 where EdU labeling was practically absent in dsBrCore-treated specimens, in comparison
346 with controls (Fig. 3C). Interestingly, the distal end of the CuP vein, where there is no
347 cell division, disappeared thereafter, on day 6, at the maximum peak of ecdysone,
348 therefore forming the characteristic notch of the BR-C knockdowns (Fig. 2B, D, F, H

349 and Supplementary Fig. S3). In the subsequent stage of tissue growth without cell
350 division, from the end of day 6 to the ecdysis, on day 8, differences between dsBrCore-
351 treated specimens and controls were not apparent in either the forewing or the hindwing
352 buds. We also used EdU labeling to study wing bud cell division around the 20E peak of
353 N5 in specimens that had been treated with two doses of dsBrCore on days 0 and 3 of
354 N4. Results showed that cell division was lower in dsBRCore-treated specimens than in
355 controls (dsMock-treated), both in the forewing and in the hindwing buds (results not
356 shown), as occurred in N6.

357

358 *3.4. Functions of individual BR-C isoforms in B. germanica*

359 All BR-C isoforms, from Z1 to Z6, are expressed simultaneously, although at
360 different levels, and show the same pattern (Fig. 1C), suggesting that all of them
361 contribute to the same functions in post-embryonic development. However, we aimed to
362 test this conjecture by carrying out isoform-specific RNAi experiments on all isoforms.
363 Treatments were carried out in N5, by injecting two doses of 3 µg of the corresponding
364 BR-C dsRNA (dsBrZ1 to dsBrZ6), one on day 0 and the other on day 3. Controls were
365 equivalently treated with dsMock.

366 Transcript depletion of the specifically targeted isoform was measured on the
367 wing pads on day 0 of N6. Transcript levels of all other non-targeted isoforms were also
368 measured as a control of RNAi specificity. Results (Fig. 4A-F) show that, in general,
369 individual isoform RNAi experiments were isoform-specific in terms of transcript
370 depletion. Treatment with dsBrZ3 reduced BR-C Z3 mRNA levels, but differences with
371 respect to the corresponding controls were not statistically significant. This treatment
372 also tended to reduce BR-C Z2 mRNA levels and, intriguingly, tended to increase the
373 mRNA levels of BR-C Z4, BR-C Z5 and BR-C Z6 (Fig. 4B). It is also worth noting that
374 treatment with dsBrZ4 significantly reduced BR-C Z4 mRNA levels, as expected, but
375 also those of BR-C-Z5 (Fig. 4D).

376 In terms of phenotype, all specimens in all isoform-specific RNAi experiments
377 molted normally to N6 and then to adult. A detailed examination of the external
378 morphology of the adult was then performed and differences with respect to controls
379 were only noticed in the wings of specimens treated with dsBrZ2 and dsBrZ6.
380 Concerning dsBrZ2-treated specimens (n = 27), 18 of them (67%) had only the A defect
381 (Fig. 4G); 1 (4%) showed only the B defect; and 7 (26%) had no visible defects. No
382 significant differences were observed in wing sizes between treated specimens and

383 controls, neither in the hindwing nor the forewing. The hindwing phenotype resembles
384 that obtained when depleting all isoforms simultaneously, but less marked, with less
385 penetrance and without the C defect (see Supplementary Fig. S3). All control (dsMock-
386 treated) specimens (n = 12) showed normal wing patterning except one specimen (8%)
387 that had the B defect. In the dsBrZ6-treated group (n = 25), 9 specimens (36%) showed
388 the B defect (Fig. 4H), whereas the remaining 16 were perfectly patterned. In the
389 control group (dsMock-treated) (n = 18), 2 specimens (11%) showed the B defect.

390 Specimens obtained from RNAi experiments targeting Z1 (dsBrZ1-treated, n =
391 18; dsMock-treated, n = 10), Z3 (dsBrZ3-treated, n = 24; dsMock-treated, n = 14), Z4
392 (dsBrZ4-treated, n = 16; dsMock-treated, n = 11) and Z5 (dsBrZ5-treated, n = 18;
393 dsMock-treated, N=10), had the wings well extended and correctly patterned (Fig. 4I),
394 and only a few specimens (between 0 and 14%, irrespective of the group, either in
395 treated or controls) had the B defect.

396

397 **4. Discussion**

398 *4.1. The patterns and the hormonal environment*

399 In *B. germanica*, BR-C isoforms are expressed in all nymphal stages, and
400 expression only declines in the last, pre-imaginal stage. The expression pattern is similar
401 in all individual isoforms of BR-C, although the respective abundances differ, Z2 being
402 the most abundant, followed by Z3, Z6, Z4, Z1 and Z5. Expression is more intense in
403 the wing pads, and the pattern appears to be determined by the hormonal environment:
404 maximum BR-C mRNA levels coincide with bursts of 20E production in the presence
405 of high levels of JH. The coincidence of BR-C expression peaks and those of 20E
406 reflects cause-effect relationships, as expression of BR-C is 20E-dependent [41]. Then,
407 BR-C mRNA levels decline in the last nymphal instar (N6), in parallel to JH vanishing,
408 although a small burst of expression is still observed on day 6 coinciding with a peak of
409 20E. The correspondence of BR-C and JH patterns, the induction of BR-C expression
410 by exogenous JH III, and their down-regulation after depletion of Kr-h1, suggest that JH
411 enhances BR-C expression during young nymphal instars. Therefore, the steady decline
412 observed in N6 must be due, at least in part, to the decrease of JH titer. In the
413 hemipteran *P. apterus*, treatment with a JH analogue induces ectopic expression of BR-
414 C in last nymphal instar, whereas depletion of Met expression led to a significant
415 reduction of BR-C expression [12]. These observations are in agreement with our

416 present results as Met is an early transducer of the JH signal and seems to play a role in
417 JH reception [9], also in *B. germanica* (our unpublished results).

418 Significant expression of BR-C in young nymphal instars has been reported in
419 the hemimetabolous species *O. fasciatus* [29] and *P. apterus* [12]. Conversely, BR-C
420 expression in holometabolous species is quantitatively relevant only in the larva-pupa
421 transition. This includes *D. melanogaster* [25], *M. sexta* [25], *B. mori* [42] and *T.*
422 *castaneum* [11, 27, 28]. Data from holometabolous species suggest that the onset of BR-
423 C expression occurs after a small burst of 20E produced in the absence of JH at the end
424 of the last larval instar. In *M. sexta*, BR-C transcripts appear at the end of the feeding
425 stage (beginning of wandering behavior) in the epidermis of last instar larvae, when the
426 insect becomes committed to pupal differentiation. Administration of JH in this stage
427 prevents the 20E-induced expression of BR-C [43]. Later, levels of BR-C mRNA
428 decrease during the pupal stage and the pupae transform into the adult stage. In pupae,
429 exogenous JH induces the re-expression of BR-C, and the insect undergoes a second
430 pupal molt [25].

431 The expression patterns of BR-C isoforms in the thysanopterans *Frankliniella*
432 *occidentalis* and *Haplothrips brevitubus* [44], are especially interesting. Thysanopterans
433 follow an essentially hemimetabolous development, in the sense that nymphs are
434 morphologically similar to adults, but the life cycle includes 1 to 3 quiescent stages,
435 called propupae and pupae, where wing buds develop considerably and which are
436 reminiscent of the holometabolous pupal stage. This particular cycle has been
437 distinguished as neometabolism development [5]. *F. occidentalis* has two nymphal
438 stages, a propupal and a pupal stage, whereas *H. brevitubus* has two nymphal stages, a
439 propupal and two pupal stages. In both species, expression of BR-C is low in the first
440 instar nymph, peaks towards the end of the second instar nymph and decreases in the
441 propupae. Moreover, treatment of propupae with a JH analog induces the re-expression
442 of BR-C in the pupae [44]. The BR-C expression pattern, showing a peak just before the
443 transition from nymph to propupae, and the stimulatory effect of JH on BR-C
444 expression in the propupae, are reminiscent of the endocrine determinism of the pupal
445 stage in holometabolous species.

446

447 *4.2. The functions*

448 RNAi experiments in nymphs of *B. germanica* have shown that wing buds
449 experience intense cell proliferation, which is hampered in BR-C knockdowns. This
450 suggests that BR-C isoforms regulate progressive growth of wing buds during nymphal
451 life by promoting cell division. In the last nymphal instar there is a phase of cell
452 proliferation encompassed by the increasing levels of 20E that lead to the peak on day 6,
453 followed by a phase of cell growth and wing metamorphosis encompassed by the
454 decreasing levels of 20E that occur after the peak. In this metamorphic instar, cell
455 proliferation is also hampered in BR-C knockdowns, but the subsequent phase of cell
456 growth and metamorphosis is generally not affected by BR-C RNAi. Only some details
457 of vein patterning in the hindwing are affected by BR-C RNAi, including the length of
458 the CuP vein, the organization of the longitudinal and small transversal veins in the
459 anterior part of the hindwing, and the linear growth of the A-veins in the posterior part.

460 Therefore, the function of BR-C isoforms in postembryonic development of *B.*
461 *germanica* appears to be restricted to sustaining cell division in the wing buds, which
462 contributes to the final size and morphology of the adult wings, and regulation of a
463 number of details of vein patterning and length and in the hindwing. While the latter
464 function had not been described before in hemimetabolous insects, our observations on
465 wing size are equivalent to those obtained in *O. fasciatus* and *P. apterus*, where RNAi
466 treatments of BR-C hampered wing bud development in nymphs and resulted in adults
467 with reduced and wrinkled wings [12, 29]. Our observations refer to the external
468 morphology, as no anatomical examinations were carried out during the present work.
469 Thus, we cannot rule out the possibility of a possible role of BR-C factors in the
470 nervous system during metamorphosis of *B. germanica*, as occurs in *D. melanogaster*
471 [45, 46]. However, the primitive hemimetaboly exhibited by *B. germanica* suggests that
472 there are no dramatic transformations of the internal organs, as opposed to *D.*
473 *melanogaster*, whose internal anatomy is heavily reconstructed during metamorphosis.

474 In striking contrast, BR-C proteins play complex morphogenetic roles in
475 holometabolous species, leading to the formation of the pupal morphology. Pioneering
476 genetic studies in *D. melanogaster* demonstrated that BR-C null mutants, in which not
477 one of the isoforms is expressed, never molt to pupae [23, 47, 48]. Later, the use of a
478 recombinant Sindbis virus expressing a BR-C antisense RNA fragment in *B. mori*,
479 reduced endogenous BR-C mRNA levels in infected tissues and the insect did not
480 complete the larval-pupal transition [26]. More recently, experiments depleting BR-C

481 mRNA levels with RNAi have been carried out in *T. castaneum* [11, 27, 28] and in the
482 lacewing *Chrysopa perla* [28]. In all cases, RNAi treatments in larvae hampered larval-
483 pupal transformation and produced individuals with larval, pupal and adult features,
484 which indicates that BR-C isoforms promote the pupal developmental program while
485 suppressing those of the larvae and the adult.

486

487 4.3. The isoforms

488 In *D. melanogaster*, BR-C encodes four zinc-finger protein isoforms (Z1, Z2, Z3
489 and Z4), which share most of the amino-terminal region called the BRcore, but they
490 have a unique pair of zinc-fingers at their carboxy terminus [23, 24]. Moreover, the
491 common BRcore region contains a BR-C-Tramtrack-Bric-à-brac (BTB) domain
492 involved in protein-protein interactions [24]. Mutants corresponding to isoform-specific
493 regions form three complementing groups: *br* (*broad*), *rbp* (*reduced bristle number on*
494 *palpus*) and *2Bc* [47, 48]. Alleles belonging to the *npr1* (*nonpupariating1*) class of
495 mutations does not complement mutations in each of the three complementing genetic
496 functions. *npr1* mutations result in developmental arrest and lethality at pupariation; *br*⁺
497 function is required for wing and leg imaginal disc development and for tanning the
498 larval cuticle; *rbp*⁺ and *2Bc*⁺ functions are needed for larval tissues destruction and for
499 gut morphogenesis; moreover, *2Bc*⁺ is additionally required for complete closure of the
500 thoracic epidermis, and all three functions must occur for central nervous system
501 reorganization [47-50]. Mutant rescue experiments associated protein isoforms with
502 genetic functions, and revealed that there were isoform-specific functions, although with
503 some degree of redundancy [51]. Further studies in *D. melanogaster* have shown
504 specific space-temporal distributions of different BR-C isoforms, thus suggesting
505 distinct temporal function, especially in neural tissue morphogenesis [45, 46, 52].
506 Finally, the advent of RNAi allowed the functional study of individual BR-C isoforms
507 (Z1 to Z5) in *T. castaneum* metamorphosis. As in *D. melanogaster*, results pointed to
508 isoform-specific roles and partial redundancy [27, 28].

509 Our functional studies on specific isoforms revealed that depletion of BR-C Z2
510 and BR-C Z6 gave discernible phenotypes, in both cases related to wing patterning. BR-
511 C Z2 phenotype showed the CuP vein shorter and an associated notch at the wing edge
512 (defect A), and the vein/intervein patterning disorganized in the anterior part (defect B),
513 but it did not show the A-veins subdivided and incomplete (defect C). Moreover, the

514 penetrance and severity of the defects were lower in comparison with the BR-C Core
515 knockdowns, whilst wing size was practically unaffected. BR-C Z6 knockdowns
516 phenotype showed t defects B and C, but not defect A, which is the most typical in the
517 experiments depleting all isoforms simultaneously; wing size was unaffected.
518 Phenotypes obtained in RNAi experiments on BR-C Z1, BR-C Z3, BR-C Z4 and BR-C
519 Z5 were as in controls, including defect B, which seems qualitatively unspecific,
520 although, importantly, its occurrence in BRCore or BR-C Z6 knockdowns is
521 significantly higher than in controls. The relatively poor abundance of these isoforms in
522 the pool of BR-C proteins, and the generally modest efficiency of these RNAi
523 experiments in terms of transcript decrease, might explain the absence of differential
524 phenotypes. However, given that phenotypes observed in BR-C Z2 and BR-C Z6
525 knockdowns encompass all the defects observed in BRCore knockdowns, we can
526 presume that functions of the remaining isoforms might be redundant with those of BR-
527 C Z2 and BR-C Z6.

528

529 *4.4.Conclusion: The evolution of metamorphosis at the light of BR-C*

530 The main function played by BR-C proteins in *B. germanica*, a phylogenetically
531 basal, hemimetabolous species, during post-embryogenesis is to promote wing growth
532 to reach the right size and form. Basically, this function has been conserved in the
533 hemimetabolous species *O. fasciatus* and *P. apterus*, which are phylogenetically more
534 distal than *B. germanica*. In these bugs, the wing buds are external, not embedded in a
535 cuticular wing pad pocket, and the decrease in growth and attenuation of color pattern
536 progression of BR-C knockdowns is externally visible [12, 29]. In the beetle *T.*
537 *castaneum*, RNAi of BR-C isoforms Z2 and Z3 results in pupae with shortened wings
538 [27], which indicates that functions of BR-C related to wing size are conserved in basal
539 holometabolous species. Functions of BR-C in determining wing size and form also
540 appear to be present in the extremely modified, holometabolous species of fly *D.*
541 *melanogaster*. Indeed, the name “broad” given to one of the complementation groups of
542 BR-C derives from the oval, rather than elliptic form of the wings of these mutants,
543 which were first described by Thomas H. Morgan and colleagues in 1925 [53].
544 Therefore, the functions of BR related to controlling wing size and form appear to be
545 ancestral and conserved from cockroaches to flies. The same may hold true for the
546 subtle functions related to vein patterning observed in *B. germanica*, as the classical *br*

547 mutants of *D. melanogaster* also have defects on vein length [53]. Vein patterning in
548 BR-C knockdowns of *O. fasciatus* and *P. apterus* was not reported [12, 29].

549 Another interesting feature of BR-C in *B. germanica* is that its expression is
550 enhanced by JH. Thus, both JH and BR-C mRNA levels are high in young nymphal
551 instars and decrease in parallel during the last nymphal instar, prior to metamorphosis.
552 This contrasts with the situation found in holometabolous species, where JH inhibits
553 BR-C expression in young larvae, and so high levels of JH correlate with low levels of
554 BR-C expression [12].

555 A number of theories have been proposed to explain the evolutionary transition
556 from hemimetaboly to holometaboly [4, 54]. A classic theory originally argued by
557 Lubbock [55] and formalized by Berlese [56], proposes that the larvae of
558 holometabolous species arose by “de-embryonization”, so that it was a sort of free
559 living, often vermiform embryo. The “de-embryonization” theory was resuscitated and
560 reinforced with modern endocrine data by Truman and Riddiford [54], who proposed
561 that the holometabolous larva corresponds to the latest hemimetabolous embryonic
562 stage that the latter authors called the pronymph, and that the origin of larval form
563 would be explained by a shift in JH titers, from late embryonic stages in
564 hemimetabolous species to earlier stages in holometabolous insect embryos. Thus, in
565 postembryonic stages of holometabolous species, only when JH declines in the final
566 larval instar does extensive morphogenesis resume and lead to differentiation of the
567 pupa [57].

568 While this theory still is under debate [4], our present results show that, in a
569 basal hemimetabolous species, JH enhances the expression of BR-C in young nymphs
570 and that BR-C factors promote wing growth during nymphal life and refine wing
571 patterning at metamorphosis, which contrasts with the endocrine regulation and
572 complex functions observed in holometabolous species, as previously described in
573 classical insect models. We propose that in the evolution from hemimetaboly to
574 holometaboly, at least two key innovations appeared that affected BR-C and post-
575 embryonic morphological development. The first was a shift of JH action, from
576 stimulatory (as in present hemimetabolous species) to inhibitory (present
577 holometabolous species) of BR-C expression, during young stages. Thus, BR-C
578 expression had become inhibited during young larvae in holometabolous ancestors, with
579 the resulting suppression of growth and development of BR-C-dependent tissues, for

580 example the wing bud. The second great innovation was an expansion of functions,
581 from one specialized in wing development and details of vein patterning, as in present
582 hemimetabolous species, to a larger array of morphogenetic functions, which
583 culminated with the pupal-specifier role that operates in present holometabolous
584 species, from the basal *T. castaneum* to the distal *D. melanogaster* (Fig. 5).
585 Paradoxically, the number of isoforms decreased from six to four in the evolution from
586 cockroaches to flies, while their functions dramatically expanded.

587 The case of thysanopterans is very interesting because they show the so-called
588 neometabolous development [5], with a life cycle including quiescent “propupal” and
589 “pupal” stages that are reminiscent of the holometabolous pupae. The studies in *F.*
590 *occidentalis* and *H. brevitubus* of Minakuchi et al. [44] have shown that BR-C mRNA
591 levels are very low in young instars and show an acute peak around the formation of the
592 propupae, as occurs in holometabolous species, suggesting that BR-C expression in
593 thysanopterans is hormonally regulated and specified as in holometabolous species.
594 Reconstructions of insect phylogeny suggest that paraneopterans ((thysanopterans +
595 hemipterans)+(psocopterans and phthirapterans)) are the sister group of Holometabola
596 [58]. If so, then the first steps toward the innovation of the pupal stage, including the
597 endocrine determination, might have occurred in the ancestor of Paraneoptera +
598 Holometabola. Interestingly, hemipterans also contain representatives of neometabolous
599 development in the Sternorrhyncha [4, 5]. Our hypothesis contemplates that other
600 Hemipterans, and Psocopterans and Phthirapterans would have lost the ability to
601 produce preimaginal quiescent stages in their life cycles. Whichever the case, although
602 natural selection was able to make a first attempt to invent a sort of pupa in the ancestor
603 of the Paraneoptera + Holometabola, the invention was fully perfected in the lineage of
604 Holometabola judging by the endless forms most beautiful that stand today in this insect
605 superorder.

606

607 **Acknowledgement**

608 Financial support for this research was provided by the Spanish MICINN (grant
609 CGL2008-03517/BOS to X.B. and predoctoral fellowship to J.L.) and by the CSIC
610 (grant 2010TW0019, from the Formosa program, to X.B.). J.-H.H received a grant from
611 the National Research Council (Taiwan) to work in the Institute of Evolutionary
612 Biology, in Barcelona. Thanks are also due to Maria-Dolors Piulachs for helpful

613 discussions, and to José Martínez for helping in the experimental work.

614

615 **Appendix A. Supplementary data**

616 Supplementary data to this article can be found online at doi: XXX

617

618

619 **Figure legends**

620

621 **Fig. 1.** Expression of BR-C mRNA in *Blattella germanica* female. (A) Joint expression
622 of all isoforms in the whole body in selected days of the 6 nymphal instars: N1 to N6.
623 (B) Joint expression of all isoforms in the mesonotum and metanotum wing pads in
624 selected days of N4, N5 and N6. Concentration patterns of hemolymph juvenile
625 hormone (JH) III and 20-hydroxyecdysone (20E) are indicated below, according to
626 previously published data [33, 40]. (C) Expression of individual BR-C isoforms (Z1 to
627 Z6) in the wing pads on selected days of N6. (D) Effect of the application of 20 µg of
628 JH III. The hormone was administered on freshly emerged N6 and BR-C mRNA levels
629 were measured 2, 4 and 6 days later. (E) Effect of Kr-h1 depletion by RNAi on N4 and
630 N5. Two doses (3 µg each) of dsKr-h1 (treated) or dsMock (control) were administered
631 on N4 and N5 (on days 0 and 3 in both cases), and BR-C mRNA levels were measured
632 on day 4 in the experiments of N4, and on day 6 in the experiments of N5. Data is
633 represented as the mean ± SEM, and are indicated as copies of BR-C mRNA per 1,000
634 copies of BgActin-5c. Each point represents 3-6 biological replicates, except in panel C,
635 in which data represent one replicate per point. In panels D and E data are normalized
636 against control females (arbitrary reference value = 1) and the asterisk indicates
637 statistically significant differences with respect to controls ($p < 0.05$), according to the
638 REST software tool [31].

639

640 **Fig. 2.** Phenotype obtained after depleting all BR-C isoforms by RNAi in *Blattella*
641 *germanica*. (A-B) Effect of a single 3 µg-dose of dsMock (control) or dsBR-core
642 (treated) administered on day 0 of N5: BR-C mRNA levels on day 6 of N5 and on day 0
643 of N6 (A); adult phenotype (habitus, forewing and hindwing) (B). (C-D) Effects of two
644 doses of 3 µg each of dsBR-core administered on day 0 and day 3 of N5: BR-C mRNA
645 levels on day 0 of N6 (C); extended wings and wrinkled wings phenotype (D). (E-F)
646 Effects of two 3 µg-doses of dsBR-core administered on day 0 and day 3 of N4: BR-C
647 mRNA levels on day 0 of N5 (E); extended wings and wrinkled wings phenotype (F).
648 (G-H) Effects of two 3 µg-doses of dsMock (control) or dsBR-core (treated)
649 administered on day 0 and day 3 of N6: BR-C mRNA levels on day 6 of N6 (G); adult
650 phenotype of controls and treated specimens (H). Data in (A), (C), (E) and (G) represent

651 3 biological replicates (mean \pm SEM), are indicated as copies of BR-C mRNA per 1,000
652 copies of BgActin-5c, and are normalized against control females (arbitrary reference
653 value = 1); the asterisk indicates statistically significant differences with respect to
654 controls ($p < 0.05$), according to the REST software tool [31]. Arrows indicate the notch
655 provoked by a shortening of the CuP vein, and the arrowhead indicates disorganized
656 vein/intervein patterning in the anterior part of the hindwing. Note that the late defect
657 appeared also in controls (H).

658

659 **Fig. 3.** Development of wing buds in control and BR-C knockdown specimens of
660 *Blattella germanica*. (A) Double labeling EdU (discrete red spots) and DAPI (blue
661 color) of a hindwing bud of untreated females on days 5, 6 and 7 of the last nymphal
662 instar (N6). (B) EdU-DAPI double labeling of a forewing bud of females that were
663 treated with two doses of dsBrCore (treated) or of dsMock (control) administered on
664 days 0 and 3 of N5, and photographed on days 5 and 6 of N6. (C) EdU-DAPI double
665 labeling of a hindwing bud of females that were treated as in (B) and photographed on
666 day 5 of N6; the pictures show the region corresponding to the distal end of the CuP
667 vein (yellow oval).

668

669 **Fig. 4.** Effects obtained after depleting each BR-C isoform, from Z1 to Z6, individually,
670 by RNAi in *Blattella germanica*. (A-F) Transcript levels of the targeted and the other
671 isoforms measured in the mesonotum and metanotum wing pads on the day 0 of N6.
672 Two 3- μ g doses of dsBrZ2 (A), dsBrZ3 (B), dsBrZ6 (C), dsBrZ4 (D), dsBrZ1 (E) or
673 dsBrZ5 (F) administered on days 0 and 3 of N5; control received an equivalent
674 treatment with dsMock; data represent 3 biological replicates (mean \pm SEM) and are
675 indicated as copies of the individual BR-C isoforms mRNA per 1,000 copies of
676 BgActin-5c; the asterisk indicates statistically significant differences with respect to
677 controls ($p < 0.05$), according to the REST software tool [31]. (G-I) Adult hindwing
678 phenotype studied 3 days after the imaginal molt, from a dsBrZ2-treated specimen (G),
679 a dsBrZ6-treated specimen (H), and from a control specimen treated with dsMock. The
680 arrow indicates the main defects: the notch at the end of the CuP vein in G and the vein
681 pattern disorganized in the anterior part of the wing in H.

682

683 **Fig. 5.** BR-C and the evolution of insect metamorphosis. In the transition from
684 hemimetaboly to holometaboly, the regulation and functions of BR-C would have
685 experienced two main changes. First, a shift of JH action on BR-C expression, from
686 stimulatory in hemimetabolous to inhibitory in holometabolous species. Second, an
687 expansion of functions, from controlling wing pad growth by cell proliferation along
688 nymphal instars, and regulating subtle features of vein development and patterning
689 (hemimetabolous), to regulating pupal formation and inhibiting adult features at the end
690 of the larval life (holometabolous).
691

692 **References**

- 693 [1] C. Darwin, The origin of species by means of natural selection, or the
694 preservation of favoured races in the struggle for life, John Murray, London, 1872.
- 695 [2] D. Grimaldi, M.S. Engel, Evolution of the insects, Cambridge University Press,
696 Cambridge, 2005.
- 697 [3] P. Hammond, Species inventory, in: B. Groombridge (Ed.) Global biodiversity,
698 Chapman and Hall, London, 1992, pp. 17-39.
- 699 [4] X. Belles, Origin and Evolution of Insect Metamorphosis, in: Encyclopedia of
700 Life Sciences, John Wiley and Sons, Ltd., Chichester, 2011.
- 701 [5] F. Sehnal, P. Svacha, J. Zrzavy, Evolution of insect metamorphosis, in: L.I.
702 Gilbert, J.R. Tata, B.G. Atkinson (Eds.) Metamorphosis, Academic Press, San Diego,
703 1996, pp. 3-58.
- 704 [6] J.W. Truman, L.M. Riddiford, Endocrine insights into the evolution of
705 metamorphosis in insects, Annu. Rev. Entomol. 47 (2002) 467-500.
- 706 [7] L.M. Riddiford, How does juvenile hormone control insect metamorphosis and
707 reproduction?, Gen. Comp. Endocrinol. (2012) (in press).
- 708 [8] M. Jindra, S.R. Palli, L.M. Riddiford, The Juvenile Hormone Signaling Pathway
709 in Insect Development, Annu. Rev. Entomol. (2012) (in press).
- 710 [9] J.P. Charles, T. Iwema, V.C. Epa, K. Takaki, J. Rynes, M. Jindra, Ligand-binding
711 properties of a juvenile hormone receptor, Methoprene-tolerant, Proc. Natl. Acad. Sci.
712 U.S.A. 108 (2011) 21128-21133.
- 713 [10] B. Konopova, M. Jindra, Juvenile hormone resistance gene Methoprene-tolerant
714 controls entry into metamorphosis in the beetle *Tribolium castaneum*, Proc. Natl. Acad.
715 Sci. U.S.A. 104 (2007) 10488-10493.
- 716 [11] R. Parthasarathy, A. Tan, H. Bai, S.R. Palli, Transcription factor broad
717 suppresses precocious development of adult structures during larval-pupal
718 metamorphosis in the red flour beetle, *Tribolium castaneum*, Mech. Dev. 125 (2008)
719 299-313.
- 720 [12] B. Konopova, V. Smykal, M. Jindra, Common and distinct roles of juvenile
721 hormone signaling genes in metamorphosis of holometabolous and hemimetabolous
722 insects, PloS One 6 (2011) e28728.
- 723 [13] C. Minakuchi, X. Zhou, L.M. Riddiford, Kruppel homolog 1 (Kr-h1) mediates
724 juvenile hormone action during metamorphosis of *Drosophila melanogaster*, Mech.
725 Dev. 125 (2008) 91-105.
- 726 [14] C. Minakuchi, T. Namiki, T. Shinoda, Kruppel homolog 1, an early juvenile
727 hormone-response gene downstream of Methoprene-tolerant, mediates its anti-
728 metamorphic action in the red flour beetle *Tribolium castaneum*, Dev. Biol. 325 (2009)
729 341-350.
- 730 [15] J. Lozano, X. Belles, Conserved repressive function of Kruppel homolog 1 on
731 insect metamorphosis in hemimetabolous and holometabolous species, Sci. Rep. 1
732 (2011) 163.
- 733 [16] K. King-Jones, C.S. Thummel, Nuclear receptors--a perspective from
734 *Drosophila*, Nat. Rev. Genet. 6 (2005) 311-323.

735 [17] Y. Nakagawa, V.C. Henrich, Arthropod nuclear receptors and their role in
736 molting, *FEBS J.* 276 (2009) 6128-6157.

737 [18] C.S. Thummel, Ecdysone-regulated puff genes 2000, *Insect Biochem. Mol. Biol.*
738 32 (2002) 113-120.

739 [19] V.P. Yin, C.S. Thummel, Mechanisms of steroid-triggered programmed cell
740 death in *Drosophila*, *Semin. Cell Dev. Biol.* 16 (2005) 237-243.

741 [20] J. Cruz, C. Nieva, D. Mane-Padros, D. Martin, X. Belles, Nuclear receptor
742 BgFTZ-F1 regulates molting and the timing of ecdysteroid production during nymphal
743 development in the hemimetabolous insect *Blattella germanica*, *Dev. Dyn.* 237 (2008)
744 3179-3191.

745 [21] D. Mane-Padros, F. Borrás-Castells, X. Belles, D. Martin, Nuclear receptor HR4
746 plays an essential role in the ecdysteroid-triggered gene cascade in the development of
747 the hemimetabolous insect *Blattella germanica*, *Mol. Cell Endocrinol.* 348 (2012) 322-
748 330.

749 [22] D. Martin, O. Maestro, J. Cruz, D. Mane-Padros, X. Belles, RNAi studies reveal
750 a conserved role for RXR in molting in the cockroach *Blattella germanica*, *J. Insect*
751 *Physiol.* 52 (2006) 410-416.

752 [23] C.A. Bayer, B. Holley, J.W. Fristrom, A switch in broad-complex zinc-finger
753 isoform expression is regulated posttranscriptionally during the metamorphosis of
754 *Drosophila* imaginal discs, *Dev. Biol.* 177 (1996) 1-14.

755 [24] P.R. DiBello, D.A. Withers, C.A. Bayer, J.W. Fristrom, G.M. Guild, The
756 *Drosophila* Broad-Complex encodes a family of related proteins containing zinc fingers,
757 *Genetics* 129 (1991) 385-397.

758 [25] X. Zhou, L.M. Riddiford, Broad specifies pupal development and mediates the
759 'status quo' action of juvenile hormone on the pupal-adult transformation in *Drosophila*
760 and *Manduca*, *Development* 129 (2002) 2259-2269.

761 [26] M. Uhlirova, B.D. Foy, B.J. Beaty, K.E. Olson, L.M. Riddiford, M. Jindra, Use
762 of Sindbis virus-mediated RNA interference to demonstrate a conserved role of Broad-
763 Complex in insect metamorphosis, *Proc. Natl. Acad. Sci. U.S.A.* 100 (2003) 15607-
764 15612.

765 [27] Y. Suzuki, J.W. Truman, L.M. Riddiford, The role of Broad in the development
766 of *Tribolium castaneum*: implications for the evolution of the holometabolous insect
767 pupa, *Development* 135 (2008) 569-577.

768 [28] B. Konopova, M. Jindra, Broad-Complex acts downstream of Met in juvenile
769 hormone signaling to coordinate primitive holometabolous metamorphosis, *Development*
770 135 (2008) 559-568.

771 [29] D.F. Erezyilmaz, L.M. Riddiford, J.W. Truman, The pupal specifier broad directs
772 progressive morphogenesis in a direct-developing insect, *Proc. Natl. Acad. Sci. U.S.A.*
773 103 (2006) 6925-6930.

774 [30] M.D. Piulachs, V. Pagone, X. Belles, Key roles of the Broad-Complex gene in
775 insect embryogenesis, *Insect Biochem. Mol. Biol.* 40 (2010) 468-475.

776 [31] M.W. Pfaffl, G.W. Horgan, L. Dempfle, Relative expression software tool
777 (REST) for group-wise comparison and statistical analysis of relative expression results
778 in real-time PCR, *Nucleic Acids Res.* 30 (2002) e36.

- 779 [32] F. Camps, J. Casas, F.J. Sanchez, A. Messegue, Identification of juvenile
780 hormone III in the hemolymph of *Blattella germanica* adult females by gas
781 chromatography–mass spectrometry, *Arch. Insect Biochem. Physiol.* 6 (1987) 181-189.
- 782 [33] K. Treiblmayr, N. Pascual, M.D. Piulachs, T. Keller, X. Belles, Juvenile hormone
783 titer versus juvenile hormone synthesis in female nymphs and adults of the German
784 cockroach, *Blattella germanica*, *J. Insect Sci.* 6 (2006) 47.
- 785 [34] E. Gomez-Orte, X. Belles, MicroRNA-dependent metamorphosis in
786 hemimetabolous insects, *Proc. Natl. Acad. Sci. U.S.A.* 106 (2009) 21678-21682.
- 787 [35] X. Belles, Beyond *Drosophila*: RNAi in vivo and functional genomics in insects,
788 *Annu. Rev. Entomol.* 55 (2010) 111-128.
- 789 [36] L. Ciudad, M.D. Piulachs, X. Belles, Systemic RNAi of the cockroach
790 vitellogenin receptor results in a phenotype similar to that of the *Drosophila* yolkless
791 mutant, *FEBS J.* 273 (2006) 325-335.
- 792 [37] J.L. Maestro, X. Belles, Silencing allatostatin expression using double-stranded
793 RNA targeted to preproallatostatin mRNA in the German cockroach, *Arch. Insect
794 Biochem. Physiol.* 62 (2006) 73-79.
- 795 [38] A. Salic, T.J. Mitchison, A chemical method for fast and sensitive detection of
796 DNA synthesis in vivo, *Proc. Natl. Acad. Sci. U.S.A.* 105 (2008) 2415-2420.
- 797 [39] M.W. Pfaffl, G.W. Horgan, L. Dempfle, Relative expression software tool
798 (REST) for group-wise comparison and statistical analysis of relative expression results
799 in real-time PCR, *Nucleic Acids Res.* 30 (2002) e36.
- 800 [40] I. Romaña, N. Pascual, X. Bellés, The ovary is a source of circulating
801 ecdysteroids in *Blattella germanica* (L.) (Dictyoptera, Blattellidae), *Eur. J. Entomol.* 92
802 (1995) 93-103.
- 803 [41] F.D. Karim, G.M. Guild, C.S. Thummel, The *Drosophila* Broad-Complex plays
804 a key role in controlling ecdysone-regulated gene expression at the onset of
805 metamorphosis, *Development* 118 (1993) 977-988.
- 806 [42] A.M. Reza, Y. Kanamori, T. Shinoda, S. Shimura, K. Mita, Y. Nakahara, M.
807 Kiuchi, M. Kamimura, Hormonal control of a metamorphosis-specific transcriptional
808 factor Broad-Complex in silkworm, *Comp. Biochem. Physiol. B Biochem. Mol. Biol.*
809 139 (2004) 753-761.
- 810 [43] B. Zhou, K. Hiruma, T. Shinoda, L.M. Riddiford, Juvenile hormone prevents
811 ecdysteroid-induced expression of broad complex RNAs in the epidermis of the tobacco
812 hornworm, *Manduca sexta*, *Dev. Biol.* 203 (1998) 233-244.
- 813 [44] C. Minakuchi, M. Tanaka, K. Miura, T. Tanaka, Developmental profile and
814 hormonal regulation of the transcription factors broad and Kruppel homolog 1 in
815 hemimetabolous thrips, *Insect Biochem. Mol. Biol.* 41 (2011) 125-134.
- 816 [45] R.F. Spokony, L.L. Restifo, Broad Complex isoforms have unique distributions
817 during central nervous system metamorphosis in *Drosophila melanogaster*, *J. Comp.
818 Neurol.* 517 (2009) 15-36.
- 819 [46] B. Zhou, D.W. Williams, J. Altman, L.M. Riddiford, J.W. Truman, Temporal
820 patterns of broad isoform expression during the development of neuronal lineages in
821 *Drosophila*, *Neural Dev.* 4 (2009) 39.
- 822 [47] E.S. Belyaeva, M.G. Aizenzon, V.F. Semeshin, Kiss, II, K. Koczka, E.M.

823 Baritcheva, T.D. Gorelova, I.F. Zhimulev, Cytogenetic analysis of the 2B3-4--2B11
824 region of the X-chromosome of *Drosophila melanogaster*. I. Cytology of the region and
825 mutant complementation groups, *Chromosoma* 81 (1980) 281-306.

826 [48] I. Kiss, A.H. Beaton, J. Tardiff, D. Fristrom, J.W. Fristrom, Interactions and
827 developmental effects of mutations in the Broad-Complex of *Drosophila melanogaster*,
828 *Genetics* 118 (1988) 247-259.

829 [49] J.C. Fletcher, C.S. Thummel, The ecdysone-inducible Broad-complex and E74
830 early genes interact to regulate target gene transcription and *Drosophila* metamorphosis,
831 *Genetics* 141 (1995) 1025-1035.

832 [50] L.L. Restifo, K. White, Mutations in a steroid hormone-regulated gene disrupt
833 the metamorphosis of the central nervous system in *Drosophila*, *Dev. Biol.* 148 (1991)
834 174-194.

835 [51] C.A. Bayer, L. von Kalm, J.W. Fristrom, Relationships between protein isoforms
836 and genetic functions demonstrate functional redundancy at the Broad-Complex during
837 *Drosophila* metamorphosis, *Dev. Biol.* 187 (1997) 267-282.

838 [52] R.F. Spokony, L.L. Restifo, Anciently duplicated Broad Complex exons have
839 distinct temporal functions during tissue morphogenesis, *Dev. Genes Evol.* 217 (2007)
840 499-513.

841 [53] T.H. Morgan, C. Bridges, A.H. Sturtevant, The genetics of *Drosophila*, *Bibliogr.*
842 *Genet.* 2 (1925) 145.

843 [54] J.W. Truman, L.M. Riddiford, The origins of insect metamorphosis, *Nature* 401
844 (1999) 447-452.

845 [55] J. Lubbock, On the origin and metamorphoses of insects, Macmillan and Co. ,
846 London, 1895.

847 [56] A. Berlese, Intorno alle metamorfosi degli insetti, *Redia* 9 (1913) 121-136.

848 [57] J.W. Truman, L.M. Riddiford, The morphostatic actions of juvenile hormone,
849 *Insect Biochem. Mol. Biol.* 37 (2007) 761-770.

850 [58] W.C. Wheeler, M. Whiting, Q.D. Wheeler, J.M. Carpenter, The phylogeny of the
851 extant hexapod orders, *Cladistics* 17 (2001) 113-169.

852

853

854

Figure

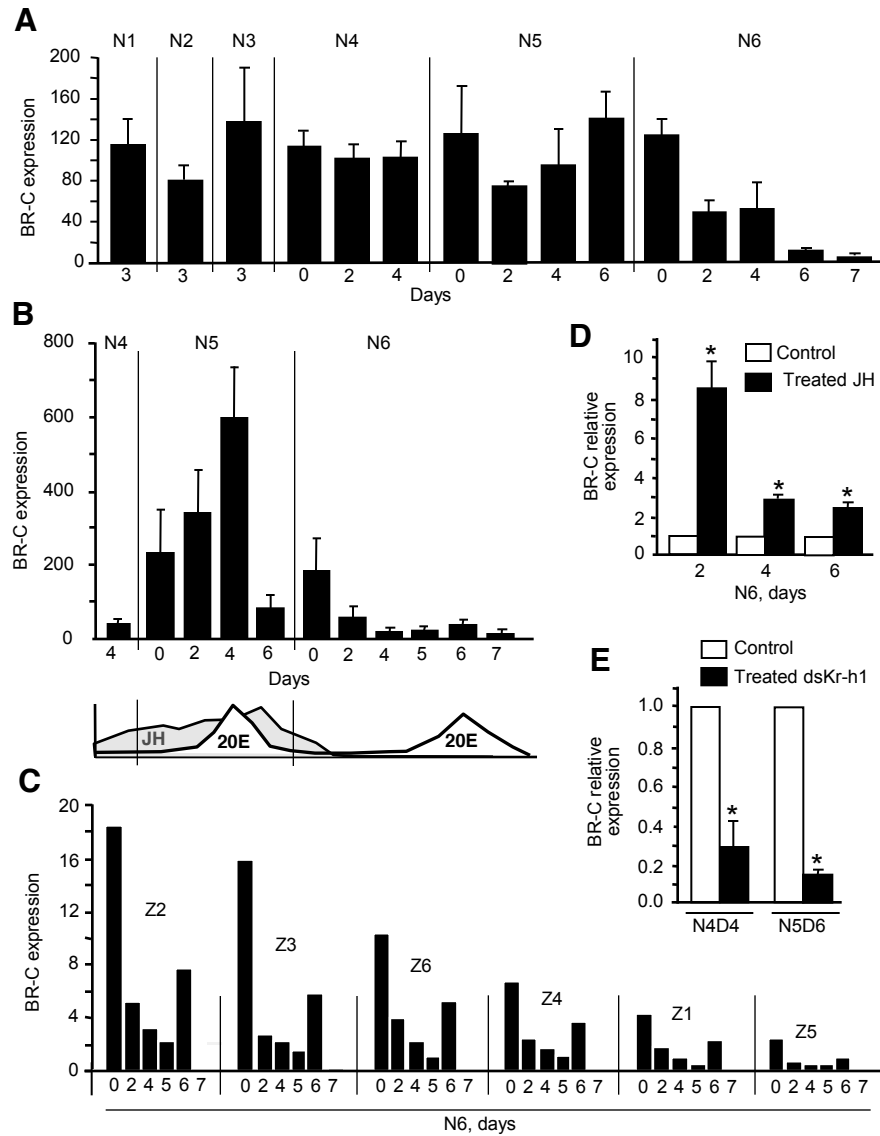


Figure 1

Figure

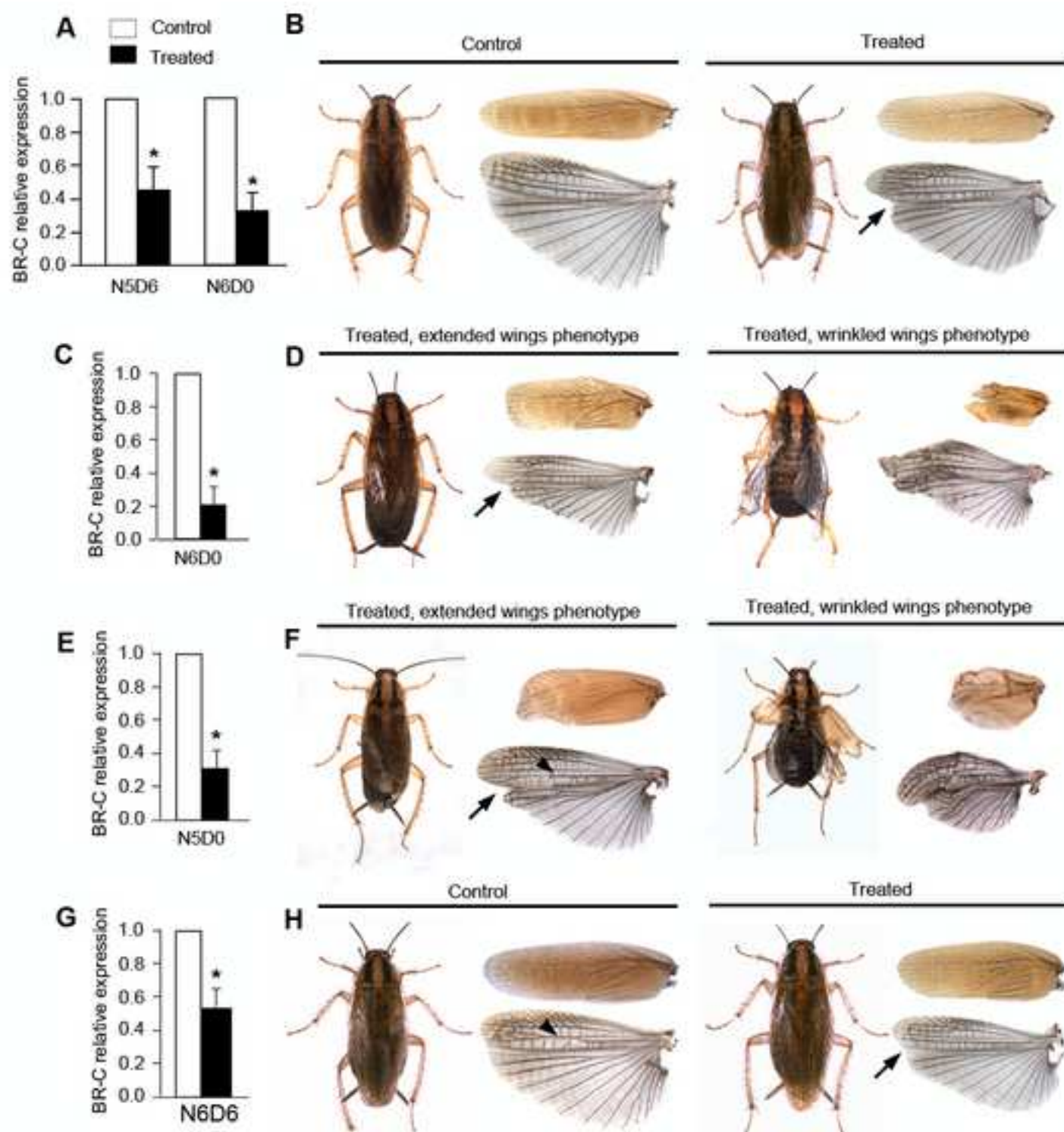
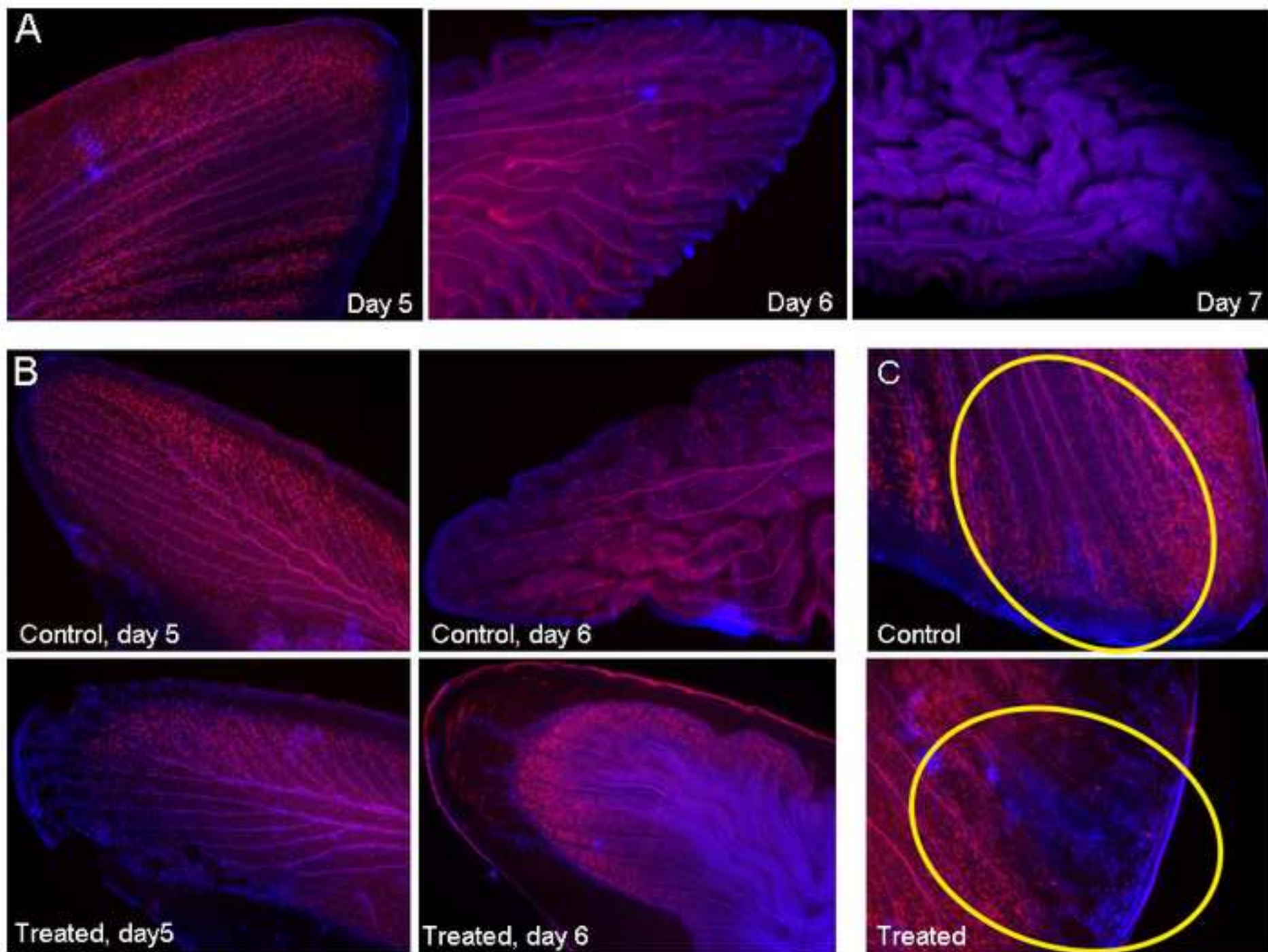
[Click here to download high resolution image](#)

Figure
[Click here to download high resolution image](#)



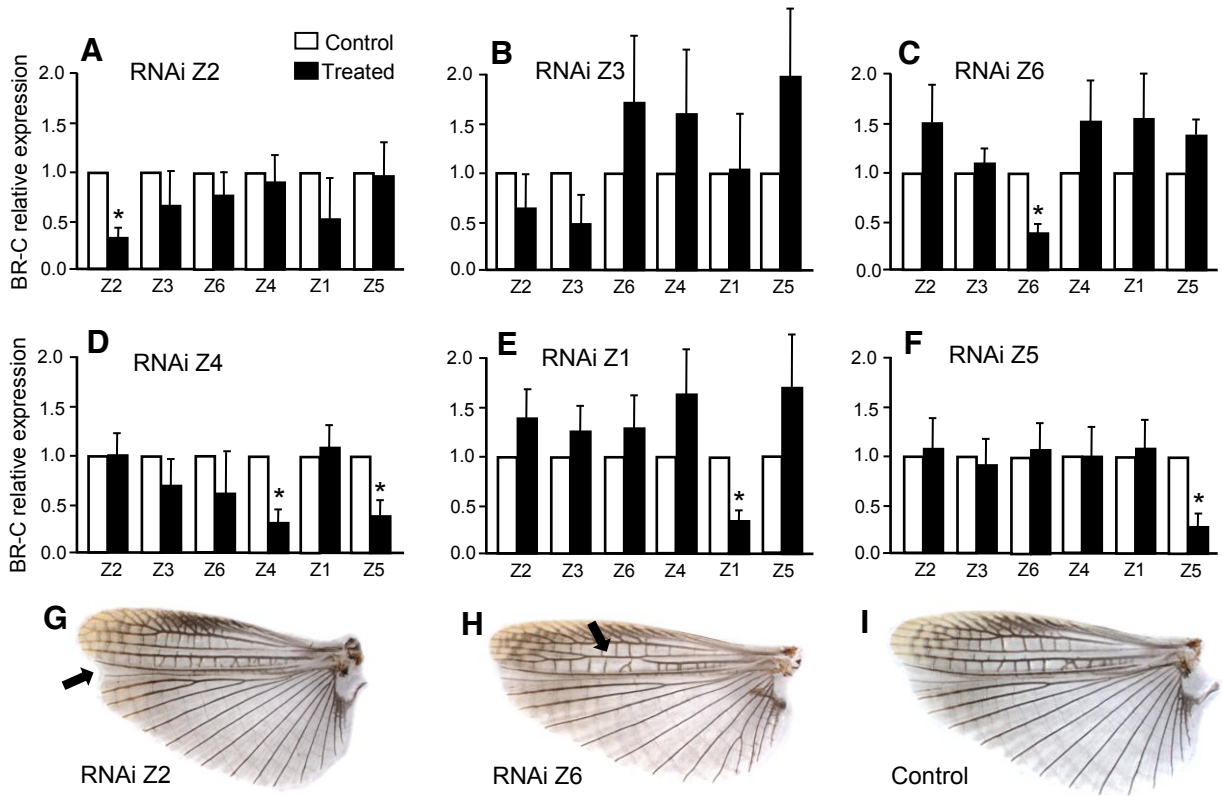


Figure 4

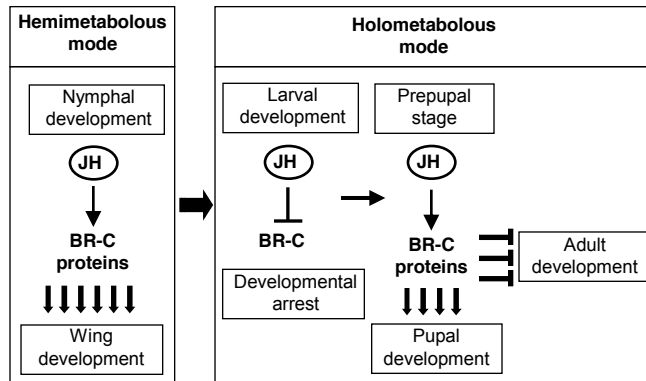


Figure 5

SUPPLEMENTARY DATA

Broad-complex, a key gene in the evolution of insect metamorphosis

Jia-Hsin Huang, Jesus Lozano, Xavier Belles

CONTENTS

Fig. S1. Comparison of the joint expression of all BR-C isoforms, with the sum of the individual expression of the 6 isoforms.

Fig. S2. Wings size of *Blattella germanica* resulting from a single dsBRCore treatment in N5 (treated) or from an equivalent treatment with dsMock (control).

Fig. S3. Venation defects in the hind wing of *Blattella germanica* resulting from a single dsBRCore treatment in N5.

Table S1. Primers used to detect the pool of all BR-C isoforms (BgBR-C) or to each isoform (BgBR-C Z1 to Z6).

Table S2. Primers used to quantify BgActin-5c.

Table S3. Primers used to generate templates with PCR for transcription of dsRNAs designed to deplete all BR-C isoforms simultaneously (dsBrCore) or specific BR-C isoforms, BgBR-C Z1 to BgBR-C Z6 (dsBrZ1 to dsBrZ6).

Fig. S1. Comparison of the joint expression of all BR-C isoforms, with the sum of the individual expression of the 6 isoforms, Z1 to Z6 represented in Figure 1C. Data are expressed as copies of BR-C mRNA per 1,000 copies of BgActin-5c.

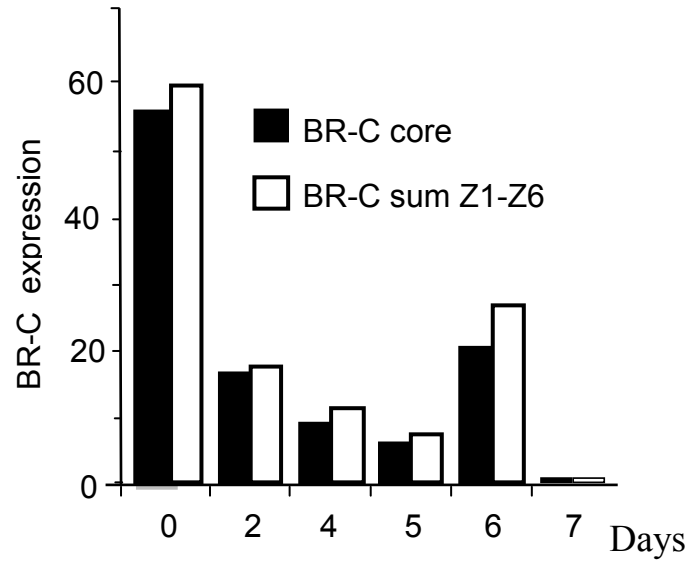


Fig. S2. Wings size of *Blattella germanica* resulting from a single dsBRCore treatment in N5 (treated) or from an equivalent treatment with dsMock (control). Top panel: Measurements carried out in the forewing (left) and hindwing (right). Bottom panel: data obtained; all values represent the mean \pm SEM (n = 34 for treated, and n = 24 for controls); asterisks indicate statistically significant differences (* P < 0.01, ** P < 0.001, *t*-test).

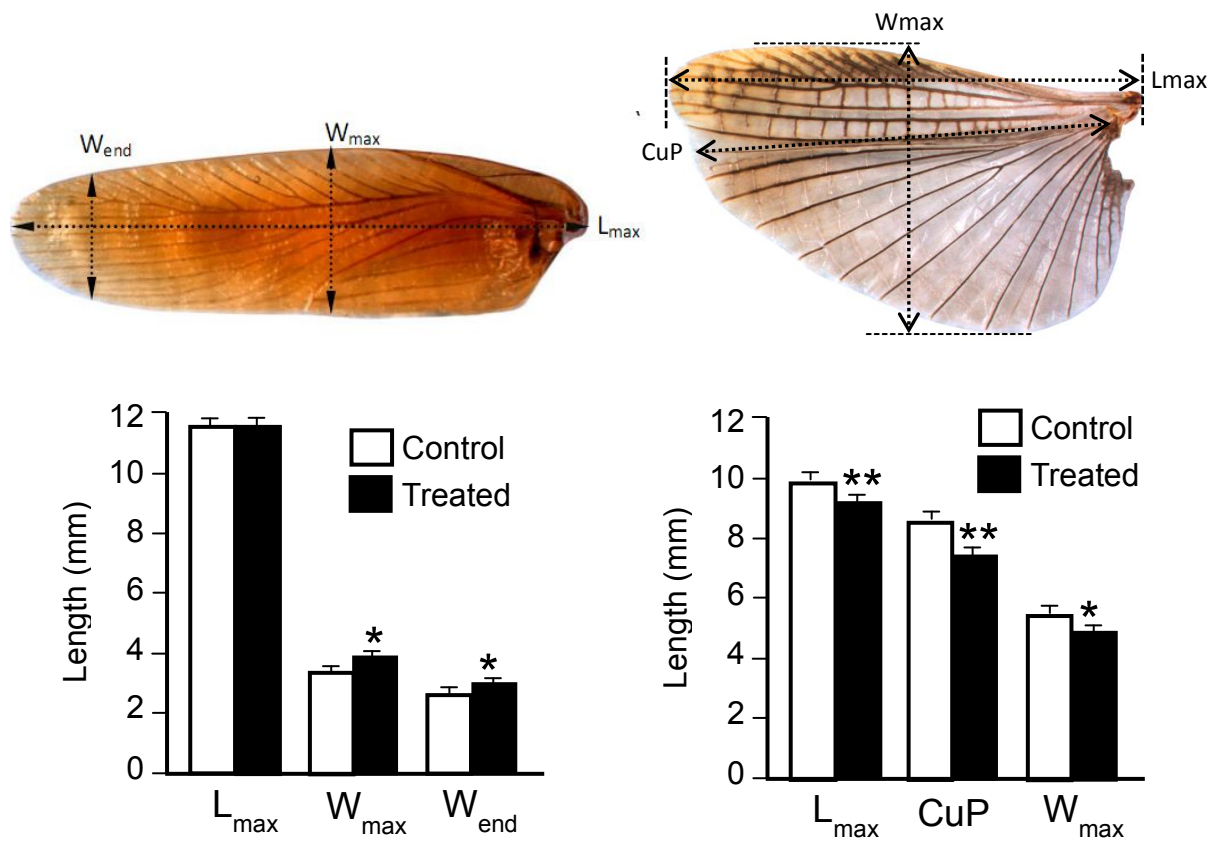
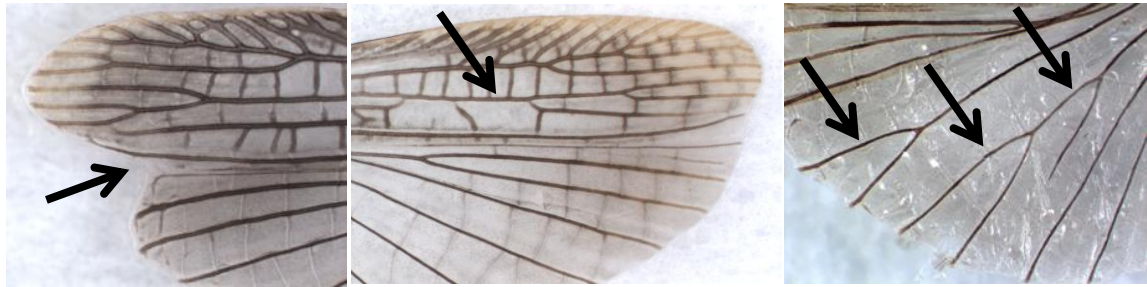


Fig. S3. Venation defects in the hind wing of *Blattella germanica* resulting from a single dsBRCore treatment in N5. Top panel: A, B and C, the three main defects observed. Bottom: penetrance of each defect or sum of defects in specimens treated with dsBRCore (treated) and in those treated with dsMock (controls).



A: Short CuP (notch) B: Vein pattern disorganized C: A-veins broken

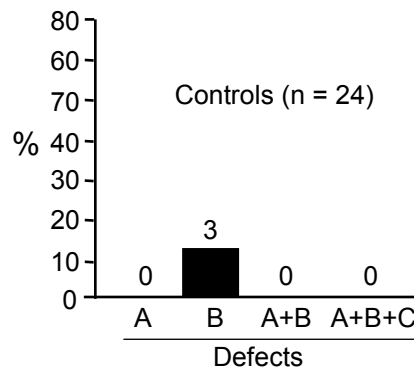
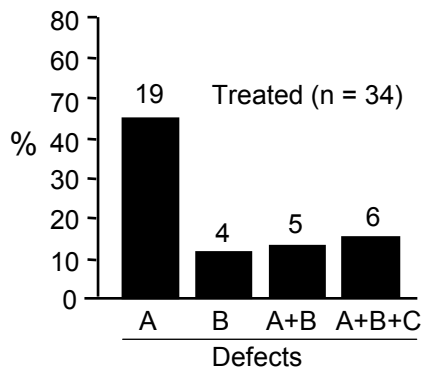


Table S1. Primers used to detect the pool of all BR-C isoforms (BgBR-C) or to each isoform (BgBR-C Z1 to Z6). The accession numbers indicated in the “Encompassed region” column refer to the sequences of the different isoforms of *Blattella germanica* BR-C.

Primer set	Forward primer (5'-3')	Reverse primer (5'-3')	Encompassed region
BgBR-C	CGGGTCGAAGGGAAAGACA	CTTGGCGCCGAATGCTGCGAT	Nucleotide 699 to 774 of FN651774
BgBR-C Z1	CTTCAAGGGAGTACGGATGG	GGCGACGTAACCTCTGTAGC	Nucleotide 1298 to 1415 of FN651774
BgBR-C Z2	CTTCAAGGGAGTACGGATGG	ATGCTTGTCTGCAACGTGTC	Nucleotide 1298 to 1429 of FN651775
BgBR-C Z3	CTTCAAGGGAGTACGGATGG	TGGAGGAGGGATGCGATAAT	Nucleotide 1298 to 1372 of FN651776
BgBR-C Z4	CTTCAAGGGAGTACGGATGG	GAGAGGTAACCTCGCCACTCG	Nucleotide 1298 to 1363 of FN651777
BgBR-C Z5	CTTCAAGGGAGTACGGATGG	GCAGTAAGGAGGTCCACTGC	Nucleotide 1298 to 1390 of FN651778
BgBR-C Z6	CTTCAAGGGAGTACGGATGG	CGCAGCTCATTTTGGATTTT	Nucleotide 1298 to 1398 of FN651779

Table S2. Primers used to quantify BgActin-5c.

Primer set	Forward primer (5'-3')	Reverse primer (5'-3')	Encompassed region
BgActin	AGCTTCCTGATGGTCAGGTGA	ACCATGTACCCTGGAATTGCCGACA	Nucleotide 96 to 186 of AJ862721

Table S3. Primers used to generate templates with PCR for transcription of dsRNAs designed to deplete all BR-C isoforms simultaneously (dsBrCore) or specific BR-C isoforms, BgBR-C Z1 to BgBR-C Z6 (dsBrZ1 to dsBrZ6). The accession numbers indicated in the “Encompassed region” column refer to the sequences of the different isoforms of *Blattella germanica* BR-C.

dsRNA	Length (bp)	Forward primer (5'-3')	Reverse primer (5'-3')	Encompassed region
dsBrCore	427	CATCAGAACAATCGCAGCATTC	TGTCCCTGAATACTGTCATGAAC	Nucleotide 744 to 1170 of FN651774
dsBrZ1	377	GCTCAGCAGGGACGTCAT	GATGAATTGAACTTACTAACTCAAGG	Nucleotide 1317 to 1693 of FN651774
dsBrZ2	285	GCTCAGCAGGGACGTCAT	CACAGGTAACACCACCTTGGAAG	Nucleotide 1317 to 1601 of FN651775
dsBrZ3	411	GCTCAGCAGGGACGTCAT	TGTGTACATGAATGGATTTTTGG	Nucleotide 1317 to 1727 of FN651776
dsBrZ6	677	GCTCAGCAGGGACGTCAT	TCTTGCCATCATGATTAAATGAC	Nucleotide 1317 to 1993 of FN651777
dsBrZ4	612	GCTCAGCAGGGACGTCAT	AAATTTGATCATGGCCTTTG	Nucleotide 1317 to 1928 of FN651778
dsBrZ1	517	GCTCAGCAGGGACGTCAT	TTGCAACCAAATTCITTAATAGG	Nucleotide 1317 to 1833 of FN651779